05911-2-T

THE UNIVERSITY OF MICHIGAN

COLLEGE OF ENGINEERING
DEPARTMENT OF ELECTRICAL ENGINEERING
SPACE PHYSICS RESEARCH LABORATORY

Scientific Report No. 1

An Acoustic Wind Measuring Technique

W. W. BUSHMAN

G. M. KAKLI

G. R. CARIGNAN

Under contract with:

National Aeronautics and Space Administration
George C. Marshall Space Flight Center
Contract No. NAS8-11054
Huntsville, Alabama

Administered through: ***July 1965***

OFFICE OF RESEARCH ADMINISTRATION • ANN ARBOR

S97.3786

THE UNIVERSITY OF MICHIGAN
COLLEGE OF ENGINEERING
Department of Electrical Engineering
Space Physics Research Laboratory

Scientific Report No. 1

AN ACOUSTIC WIND MEASURING TECHNIQUE

W. W. Bushman
G. M. Kakli
G. R. Carignan

ORA Project 05911

Under contract with:

NATIONAL AERONAUTICS AND SPACE ADMINISTRATION
GEORGE C. MARSHALL SPACE FLIGHT CENTER
CONTRACT NO. NAS8-11054
HUNTSVILLE, ALABAMA

Administered through:

OFFICE OF RESEARCH ADMINISTRATION ANN ARBOR

July 1965

TABLE OF CONTENTS

LIST OF FIGURES AND TABLES

NOTATION

A_m	Sound arrival time at the m^{th} microphone measured relative to the arrival time at the center microphone and corrected for horizontal and vertical departures of the microphone location from a horizontal cross.
A'_m	Measured arrival time at the m^{th} microphone.
$A(x)$	Functional relation between the arrival times at microphones 4,5,6,7 and the x coordinate.
$A(y)$	Functional relation between the arrival times at microphones 2,3,8,9 and the y coordinate.
δA_h	Correction in the arrival time for horizontal displacement of a microphone.
δA_z	Correction in the arrival time for vertical displacement of a microphone.
ΔA_x	Error in the measured time of arrival for microphone 4,5,6 or 7.
ΔA_y	Error in the measured time of arrival for microphone 2,3,8 or 9.
$\begin{pmatrix} a \\ b \\ c \\ d \end{pmatrix}$	Coefficients of the powers of x in A(x).
$\begin{pmatrix} a' \\ b' \\ c' \\ d' \end{pmatrix}$	Coefficients of the powers of y in A(y).
e	East
$\begin{pmatrix} F \\ G \\ H \end{pmatrix}$	Symbol for the functional representation of a system of equations used in the error analysis.
j	Index of the noise event.
J	Jacobian of the system of equations used in the error analysis.
K_x, K_y	Characteristic velocity in the x and y direction.

K_x', K_y'	Approximate characteristic velocity in the x and y direction.
L, M	Counters used in the computer solution to indicate the numbers of trials required for convergence of the solution.
n	North
$\bar{P}$	Propagation velocity vector.
P	Magnitude of the propagation velocity vector.
$\begin{pmatrix} P_x \\ P_y \\ P_z \end{pmatrix}$	x, y, z components of propagation vector.
$\bar{R}$	Position vector of the noise source in the x, y, z system.
T	Time measured along the trajectory of the vehicle referenced to the launch time.
T_j	Time of the j^{th} noise event measured along the trajectory of the vehicle referenced to the launch time.
t_j	Travel time of a sound wave from the top of the j^{th} layer to the center microphone.
Δt_i	Time interval spent by a sound wave in the i^{th} layer $(i \leq j)$
δT_j	Initial estimate of the time difference along the trajectory between the $(j-1)^{st}$ and j^{th} noise event.
$\bar{V}$	Velocity of sound vector.
V	Magnitude of velocity of sound vector.
$\begin{pmatrix} V_x \\ V_y \\ V_z \end{pmatrix}$	Components of the velocity of sound vector.
V_{avgj}	Average speed of sound in the j^{th} layer.
V_j'	Speed of sound in the j^{th} layer calculated from the sound refraction.
ΔV	Error in the speed of sound.
$\bar{W}$	Wind vector.

$\begin{pmatrix} W_x \\ W_y \\ W_{X_\ell} \\ W_{Z_\ell} \\ W_n \\ W_e \end{pmatrix}$ Horizontal wind components in the x,y; X_ℓ,Z_ℓ and n,e direction, respectively.

$\begin{pmatrix} \Delta W_x \\ \Delta W_y \end{pmatrix}$ Error in the x and y wind components.

$\begin{pmatrix} x \\ y \\ z \end{pmatrix}$ Coordinate system defined by the two legs of the microphone array with origin at the center microphone. z points up.

$\begin{pmatrix} x_j \\ y_j \\ z_j \end{pmatrix}$ Coordinates of the j^{th} noise event in the (x,y,z) system.

$\begin{pmatrix} X_\ell \\ Y_\ell \\ Z_\ell \end{pmatrix}$ Coordinates of the vehicle in the earth fixed coordinate system of the trajectory. The origin of this system is at the launch site.

$\begin{pmatrix} x_m \\ y_m \\ z_m \end{pmatrix}$ Coordinates of the m^{th} microphone in the (x,y,z) system.

z_i z coordinate of the top of the i^{th} layer $(i \leq j)$.

Δx_i, Δy_i Increments of horizontal range of the sound ray in the i^{th} layer in the (x,y,z) system.

$\begin{pmatrix} \alpha \\ \beta \\ \gamma \end{pmatrix}$ Direction cosines of the wave front normal with the x, y and z axes.

ε_1 The tolerance within which V_j' and V_{avgj} are matched.

ε_2 Increment in T.

θ Elevation angle of the wave front normal at the center microphone.

τ_j Total elapsed time from lift-off to the sound arrival of the j^{th} noise event at the center microphone.

ϕ Azimuth angle of the wave front normal at the center microphone.

Notation for Computer Output: (Tables 1 and 2)

DWX = ΔW_x

DWY = ΔW_y

J = j

KX = K_x

KY = K_y

TAU = τ

WE = W_e

WN = W_n

WX = W_x

WXL = W_{x_ℓ}

WY = W_y

WZL = W_{z_ℓ}

X = x

Y = y

Z = z

Z_{AVG} = z_{avg}

INTRODUCTION

A technique for measuring winds using the Saturn exhaust noise has been successfully employed to determine the wind profile over Cape Kennedy from ground to 85 kilometers. The technique is an extension of the Rocket-Grenade Experiment, utilizing as its sound source, rather than the grenade, the acoustic noise of the Saturn rocket exhaust.

In the Rocket-Grenade Experiment discreet sound events occur at accurately known positions, and the times and angles of arrival of these events at a ground microphone array are used to determine the atmospheric temperature and winds[1]. The use of the rocket exhaust to provide the noise events leads to a substantial difference between the two methods. The purpose of this report is to describe the technique and to present the wind profile determined during the flight of the Saturn SA-9. The method of data reduction is described and a preliminary error analysis is presented.

II. BACKGROUND

The Rocket-Grenade Experiment is described in the literature[2,3] and the meteorological results of its extensive application form the basis for a large part of man's knowledge of the atmosphere between 30 and 85 kilometers. The grenade technique is based on the dependence of the velocity of sound in a gaseous medium on the gas temperature and mass motion. By measuring the time required for a sound event to traverse from its source of known position to a microphone array on the ground and measuring its angle of arrival, the average temperature and wind between adjacent grenade detonations can be determined.

When rocket exhaust noise is used, because of its continuous nature, the time and location of a given noise event is not known, except that it occured along the trajectory. If, however, the temperature is determined independently, then the arrival angles of each of the many noise events that characterize the exhaust can be used to determine winds. A ground based array of microphones intercepts the acoustic wave front of a noise event and the time of arrival at individual microphones is used to calculate arrival angle. The noise event is traced back by an iterative process until it correctly intercepts the trajectory. Each noise event so traced leads to a wind data point, giving rise to a wind profile in a stratified atmosphere with the average wind in each layer between selected noise events.

The assumptions made for the approach described here are:

1) The vertical component of wind is negligible compared with the local speed of sound.

2) The source of sound is considered to be a point located at the nozzle of the engine or a known distance behind along the flight path. The sound wave is approximated by a plane wave at a large distance from the source.

3) The atmosphere remains in a steady state for the duration of the measurement.

III. THE EXPERIMENT

3.1 The Measurement

A cross shaped array of nine microphones was set up on the southeast point of Cape Kennedy to monitor the SA-9 flight. A minimum of three microphones are necessary to determine the arrival angle of the sound; the additional microphones provide a method of improving accuracy and afford redundancy. As shown in the error analysis, the proper use of the additional microphones eliminates first order sphericity errors from the plane wave analysis.

The size of the microphone array shown in Fig. 1 is about 1200 meters on each crossed axis. The size is based on consideration of the accuracy with which arrival times can be measured and on errors introduced by the second order sphericity term which increases with array size. The microphones are located in heavily vegetated locations to minimize local wind noise. At each microphone location, a concrete box is sunk so that its top surface is level with the surface of the ground. These boxes contain the microphones and serve as permanent survey markers. A survey was performed which defined the local geodetic network position of each microphone location to within 6 inches.

The microphones are hot wire, single chamber Helmholtz resonators tuned to about 4 cycles/sec. This low frequency characteristic is particularly well suited to extremely far field measurements since the atmosphere tends to be a low pass filter over long distances. The microphones and their amplifiers were designed at Texas Western College for use in the

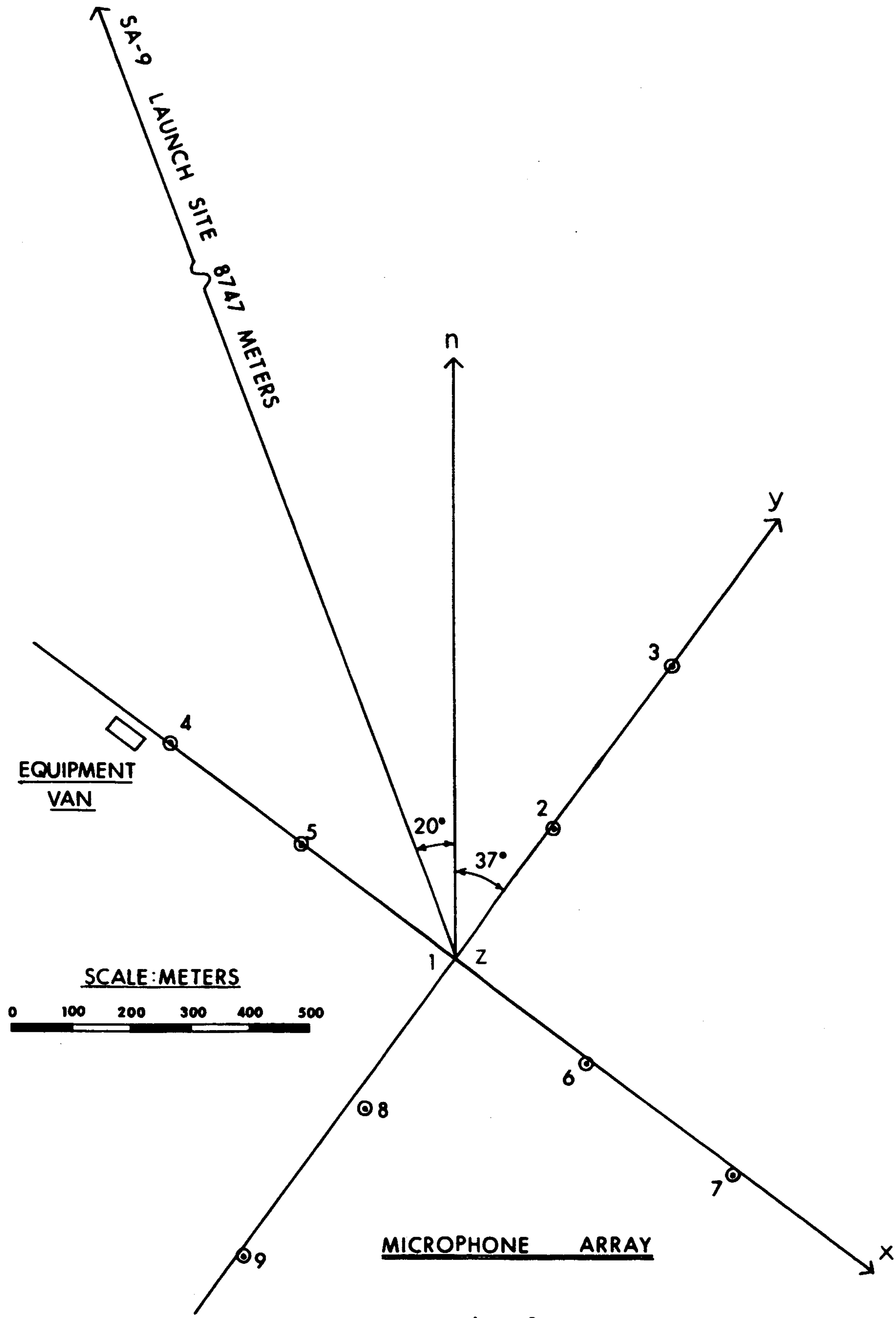
SA-9 LAUNCH SITE 8747 METERS
n
y
3
4
EQUIPMENT
VAN
2
5
20°
37°
1
Z
SCALE: METERS
0 100 200 300 400 500
6
8
7
9
MICROPHONE ARRAY
x

Fig. 1

Rocket-Grenade Experiment[4].

Fig. 2 is a block diagram of the sound ranging system. The electronic and recording equipment are housed in a van located near microphone 4. Although a location near microphone #1 would require about 2 1/2 miles less microphone cable, it was considered desirable to keep the van removed from the array to reduce the possibility of reflective interference.

The microphone outputs are recorded from before launch until 10 minutes after loss of signal. On the SA-9 flight, the microphones were located about 10 km from the launch pad. The exhaust noise was audible to the microphones from launch to more than 100 km slant range. A manually operated variable attenuator was used to maintain a proper signal level into the recording system. Fig. 3 is a 2-second record made at about 55 seconds after launch. The correlation of the microphone outputs is shown.

3.2 Theory

In the absence of local interference, the acoustical wave front of a noise event appears essentially identical to microphones at separated locations. If identical microphones are used, the output wave form of one microphone matches that of another - shifted in time. This time shift is a function of the sound arrival angle, the local speed of sound, and the microphone placement. The arrival angle can be calculated by measuring the time interval and the local speed of sound.

After the angle of arrival of a noise event is determined, the sound is ray traced backwards towards the source. The first

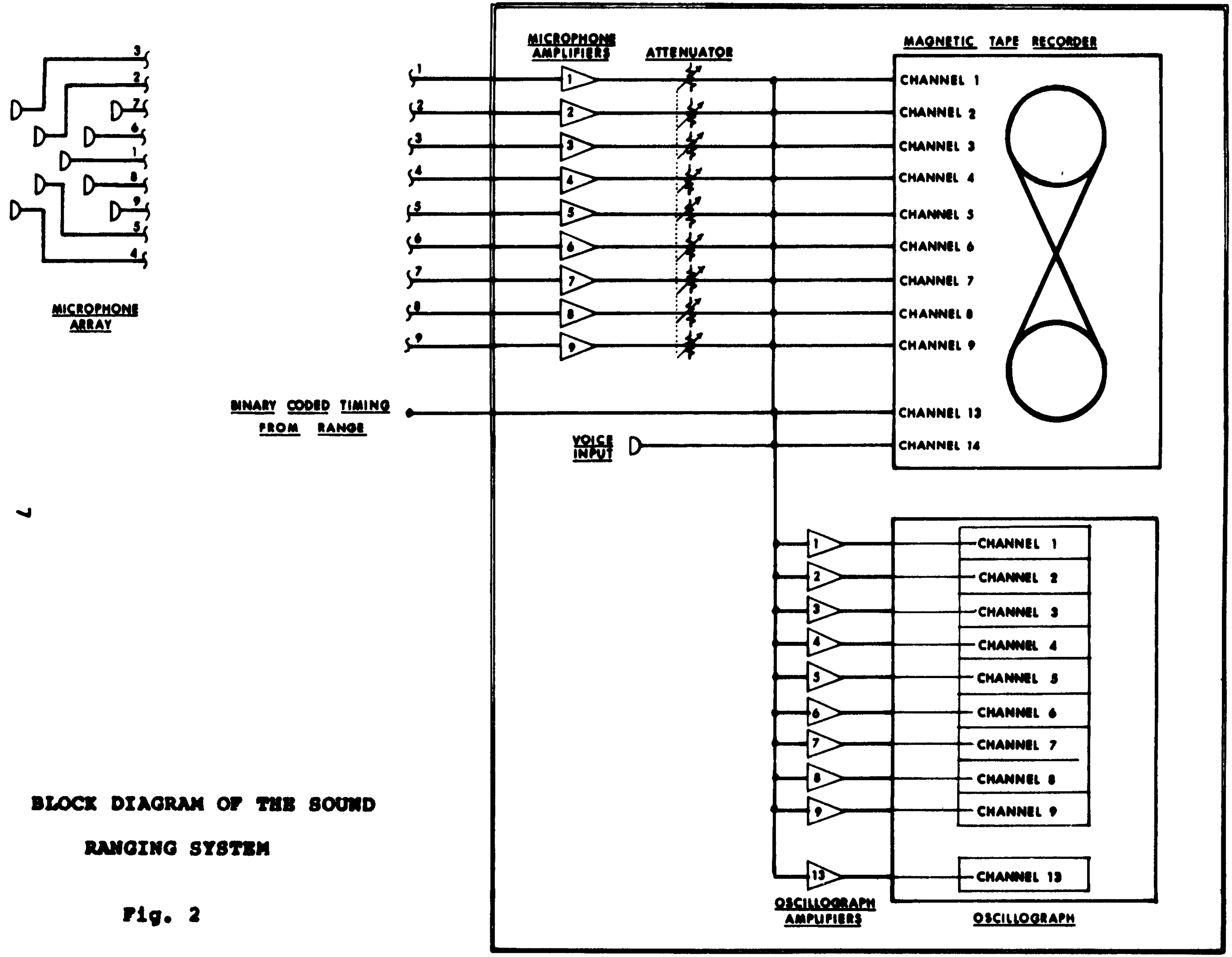

BLOCK DIAGRAM OF THE SOUND RANGING SYSTEM

Fig. 2

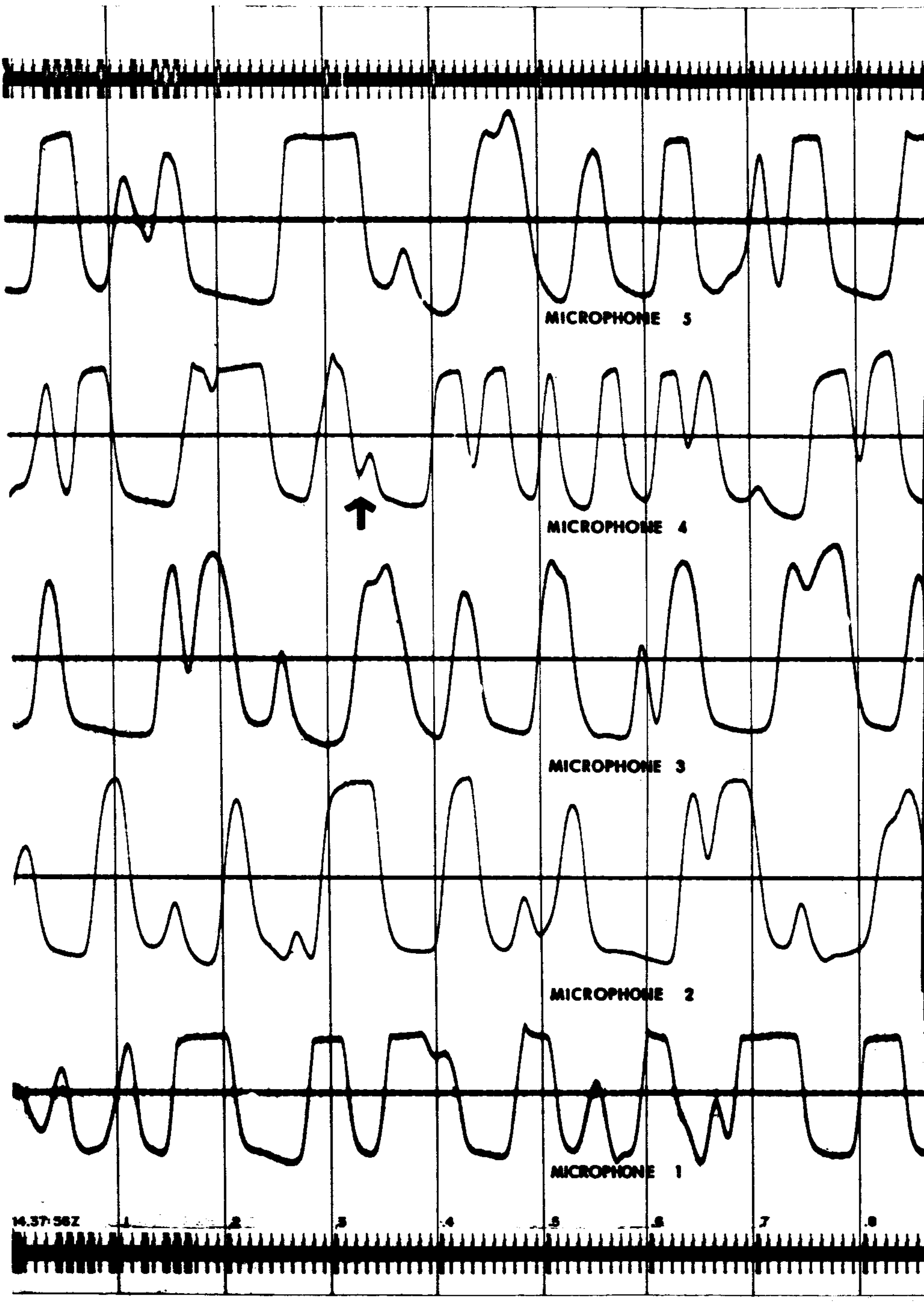

Fig. 3 Oscill
The ar

/

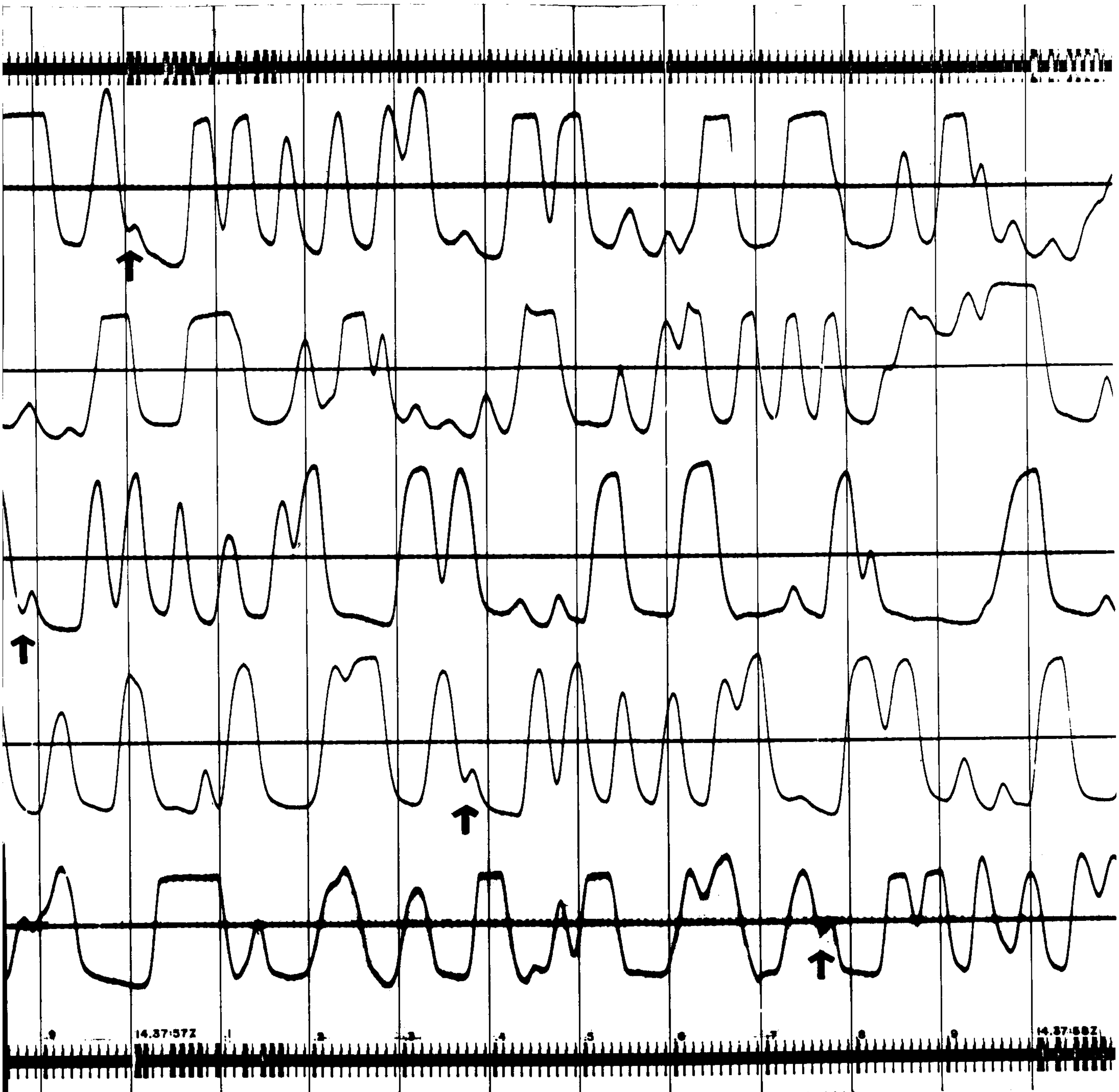

ogram of Microphones 1,2,3,4 & 5
rows locate a correlated wave form

noise events are ray traced through layers of known temperature and wind. Eventually an interval is reached between the top of the last layer of known wind and the source of sound. At this point, conventional ray tracing procedures must be abandoned since the wind is unknown; however, two independent requirements are available.

1) The sound ray must intersect the trajectory.
2) Any intersection chosen will yield a wind value. The correct intersection point must satisfy the criterion that the time of arrival of the noise event measured from launch equals the time of flight to the intersection plus the time required for the sound to travel from the intersection to the array.

These two conditions uniquely determine the coordinates of the source along the trajectory and the average wind in the interval.

IV. DATA ANALYSIS

The first step in data reduction is the cross correlation of the microphone output wave forms in order to determine the arrival times. In the analysis of the SA-9 data, this cross correlation was done manually using the method described below.

1) A group of at least ten successive waves is selected from the output of microphone 1.

2) This group of waves is identified on every other channel. The identification is made by comparison of wave shapes and periods.

3) The wave form with the sharpest peak is chosen from this group and its time of occurrance on each microphone is recorded.

After the arrival times are read, the arrival angles are written in terms of characteristic velocities along each axis, K_x and K_y. The characterisitc velocities K_x and K_y are defined as the velocities of the intersection of the wave front with the x and y axes respectively.

In terms of characteristic velocities, the elevation and azimuth angles of the normal to the wave front are

$$\theta = \cos^{-1} \frac{V_o (K_x^2 + K_y^2)^{1/2}}{K_x K_y - K_x W_{y_o} - K_y W_{x_o}} \tag{1}$$

$$\phi = \tan^{-1} \frac{K_x}{K_y} \tag{2}$$

where V_o is the velocity of sound and W_{x_o}, W_{y_o} are the x and y components of the wind at the ground.

Along each axis the arrival times at 5 microphones are measured. In the calculation of K_x and K_y all times are measured with respect to microphone No. 1, reducing this to 4 non-zero arrival times. Only one of the 4 times is necessary to define the characteristic velocity for an axis, but errors can be reduced by averaging or by writing the arrival times as a function of the distance along the axis.

$$A(x) = ax + bx^2 + cx^3 + dx^4 \qquad (3a)$$

$$A(y) = a'y + b'y^2 + c'y^3 + d'y^4 \qquad (3b)$$

Any polynomial of 4th degree or less can be used. The coefficients are computed by imposing a "least square error" restriction.

The nine microphones do not lie exactly on the two legs of a horizontal cross. Corrections in the sound arrival times due to their displacements in the horizontal and vertical directions have been derived by Otterman[5].

For horizontal correction

$$\delta Ah_m = \frac{x_m}{K_x'} = x_m \frac{(A_7' - A_4')}{x_7 - x_4} \qquad (4a)$$

$$(m = 2,3,8,9)$$

$$\delta A_{h_m} = \frac{y_m}{K_y'} = y_m \frac{(A_3' - A_9')}{y_3 - y_9} \qquad (4b)$$

$$(m = 4,5,6,7)$$

For vertical correction:

$$\delta A_{z_m} = P_z \frac{z_m}{V^2} \qquad (5)$$

$$(m = 2,3 \,........\, 9)$$

The corrected time for the m^{th} microphone, A_m, referenced to microphone #1 is:

$$A_m = A'_m - \delta A_{h_m} - \delta A_{z_m} - A_1 \tag{6}$$

$$(m = 2, 3 \ldots\ldots\ldots 9)$$

The characteristic velocities K_x and K_y are defined as follows:

$$K_x = \left(\frac{\partial X}{\partial A}\right)_o = 1/a \tag{7}$$

$$K_y = \left(\frac{\partial Y}{\partial A}\right)_o = 1/a' \tag{8}$$

Milne[6] has shown that the wave front normal of the ray reaching the microphones remains parallel to the same vertical plane throughout its propagation. For a plane wave then, the characteristic velocities of a specific sound ray are constant. Since the temperature and wind are treated as constant in any layer, the segment of the sound ray in that layer can be approximated by a straight line. The wave front, assumed plane, is refracted at each layer interface in a way analogous to the refraction of light waves. This refraction is due to a change in the magnitude of velocity of sound between layers. Further refraction occurs if wind direction and magnitude are not identical across layer boundaries.

Before the wind can be computed in any layer (j^{th}) the sound is ray traced through the previous layers where the wind has been found. The equations used for this ray tracing have been derived by Otterman for the Grenade Experiment[5]. The components of the sound velocity of the j^{th} noise event in any previous layer(i^{th}) are in terms of known quantities

$$V_{x_i} = \frac{V_{avg_i}^2}{K_{x_j} - W_{x_i} - W_{y_i} \frac{K_{x_j}}{K_{y_j}}} \tag{9a}$$

$$V_{y_i} = \frac{V_{avg_i}^2}{K_{y_j} - W_{y_i} - W_{x_i} \frac{K_{y_j}}{K_{x_j}}} \tag{9b}$$

$$P_{z_i} = (V_{avg_i}^2 - V_{x_i}^2 - V_{y_i}^2)^{1/2} \tag{9c}$$

The time spent in the i^{th} layer is

$$\Delta t_i = \frac{z_i - z_{i-1}}{P_{z_i}} \tag{10}$$

And the distance traveled is

$$\Delta x_i = \Delta t_i \ (W_{x_i} + V_{x_i}) \tag{11a}$$

$$\Delta y_i = \Delta t_i \ (W_{y_i} + V_{y_i}) \tag{11b}$$

The total time and distance through the $(j-1)^{st}$ layer is then

$$\sum_{k=1}^{j-1} \Delta t_k$$

$$\sum_{k=1}^{j-1} \Delta x_k \tag{12}$$

$$\sum_{k=1}^{j-1} \Delta y_k$$

Next to determine winds in the last layer:

The rocket position versus time function is obtained from the trajectory:

$$X_\ell = X_\ell(T)$$
$$Y_\ell = Y_\ell(T) \qquad (13)$$
$$Z_\ell = Z_\ell(T)$$

where T represents flight time or time of emittance of a noise event measured from lift-off. The coordinates X_ℓ, Y_ℓ, Z_ℓ, are then transformed to (x, y, z), the coordinate system at the center of the microphone array. From the geometry of Fig. 4, the following time and velocity equations are apparent.

Time Relationships for j^{th} Noise Event

$$\tau = T + t \qquad (14)$$

$$t = \sum_{k=1}^{j-1} \Delta t_k + \Delta t_j \qquad (15)$$

where Δt_j = the increment of time in the unknown layer.

t = total travel time of the sound from (x_j, y_j, z_j) to the array.

Velocity relationships:

$$P = \frac{[(x_j - \sum_{k=1}^{j-1} \Delta x_k)^2 + (y_j - \sum_{k=1}^{j-1} \Delta y_k)^2 + (z_j - z_{j-1})^2]^{1/2}}{\Delta t_j} \qquad (16)$$

$$P_z = \frac{z_j - z_{j-1}}{\Delta t_j} \qquad (17a)$$

$$P_x = \frac{x_j - \sum_{k=1}^{j-1} \Delta x_k}{\Delta t_j} \qquad (17b)$$

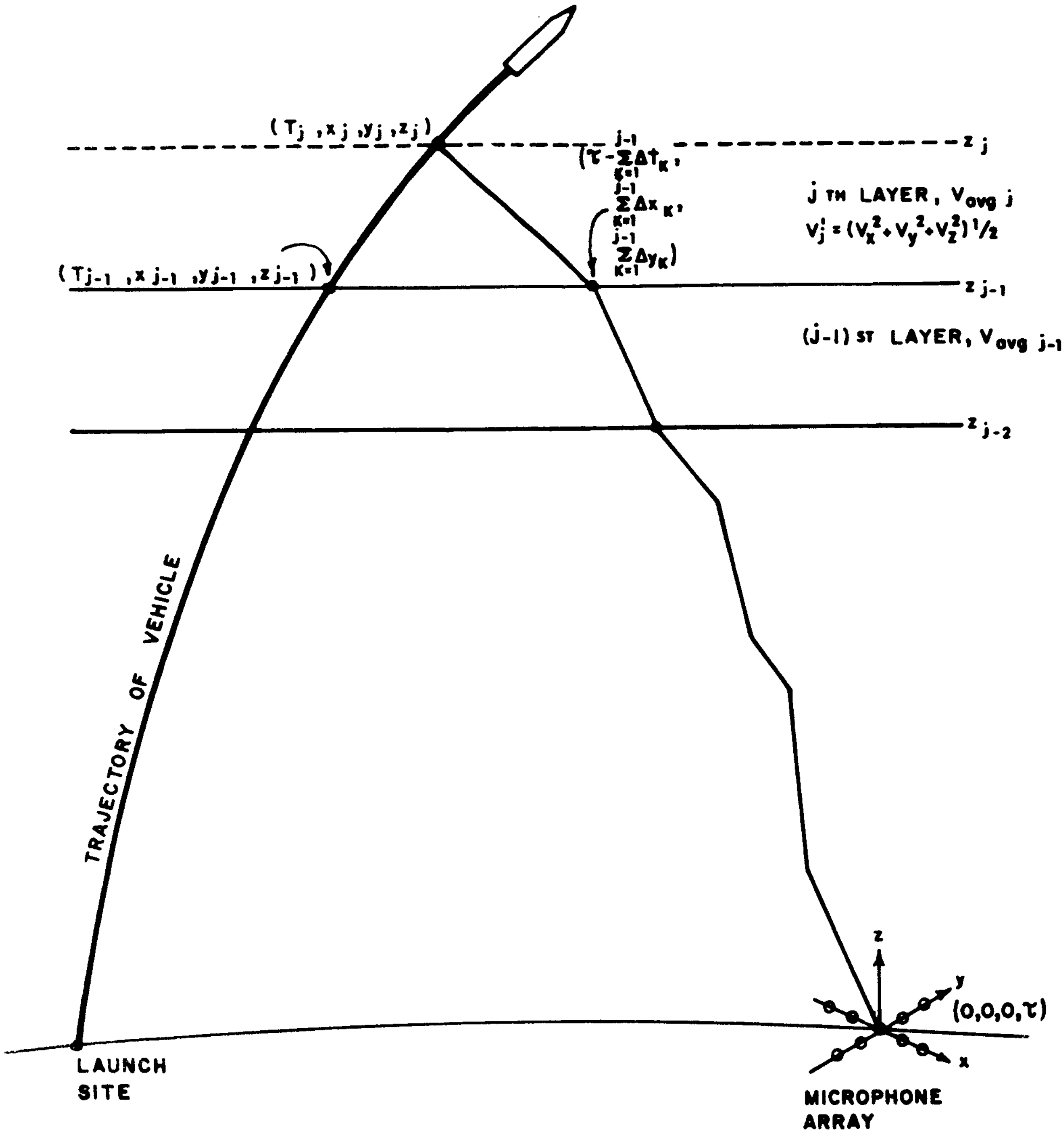

GEOMETRY OF THE WIND EXPERIMENT SHOWING TIME RELATIONSHIPS FOR THE j TH NOISE EVENT

THE SOUND IS HEARD AT THE ARRAY AT TIME τ.

Fig. 4

$$P_y = \frac{y_j - \sum_{k=1}^{j-1} \Delta y_k}{\Delta t_j} \tag{17c}$$

where P = magnitude of propagation velocity vector of the sound ray.

and P_x, P_y, P_z are components of $\overline{P}$ in the x, y, z directions, respectively.

The propagation velocity is the total velocity of the wave front traveling along the straight line path from (x_j, y_j, z_j) to

$$\sum_{k=1}^{j-1} \Delta x_k, \quad \sum_{k=1}^{j-1} \Delta y_k, \quad z_{j-1}$$

It is composed of the velocity of sound and the wind and is, therefore, not in general normal to the wave front. Thus, equations 17a, 17b, and 17c can be written as:

$$P_z = V_z \tag{18a}$$

$$P_x = V_x + W_x \tag{18b}$$

$$P_y = V_y + W_y \tag{18c}$$

W_x, W_y are the components of wind in the layer under investigation for x and y directions, respectively. (W_z is neglected). V_x, V_y, V_z are the velocity of sound components in the layer under investigation for the x, y and z directions, respectively.

For the unknown, but constant wind field in the layer between (x_j, y_j, z_j) and $\left(\sum_{k=1}^{j-1} \Delta x_k, \sum_{k=1}^{j-1} \Delta y_k, z_{j-1}\right)$ there can be only one ray path from the trajectory that will satisfy the equations (14) through (18) and the condition that characteristic velocities are constant for a given ray. Otterman[5] has derived the following expressions for V_x and V_y. These equations exemplify this directional dependence of $\overline{V}$ in any layer on the measured characteristic velocities at the array.

$$V_x = \frac{V_z^2}{K_x - P_x - P_y \frac{K_x}{K_y}} \tag{19a}$$

$$V_y = \frac{V_z^2}{K_y - P_y - P_x \frac{K_y}{K_x}} \tag{19b}$$

The magnitude of the velocity of sound can be found from:

$$V' = (V_x^2 + V_y^2 + V_z^2)^{1/2} \tag{20}$$

From these eight equations (13) through (20), position (x_j, y_j, z_j, T_j) and an average wind can be determined for the layer under investigation. These equations are solved by the procedure outlined below.

A sound is heard at the time, τ, from lift-off at the microphone array. Characteristic velocities K_x and K_y are determined and the ray is retraced to the top of the level of known temperature and wind. This point of intersection is

$$\left(\sum_{k=1}^{j-1} \Delta x_k, \sum_{k=1}^{j-1} \Delta y_k, z_{j-1} \right).$$

$\sum_{k=1}^{j-1} \Delta t_k$ is determined during the ray tracing calculation.

Next:

1) A reasonable value for T_j based upon the velocity of sound and winds in lower layers is selected. This determines coordinates x_j, y_j, z_j along the trajectory.

2) t and Δt_j are determined using equations (14) and (15).

3) Using Δt_j and the position coordinates chosen, P_z, P_x, and P_y are determined from equation (17).

4) These in turn are used in equation (19) to obtain V_x and V_y.

5) From equation (20) the magnitude of the velocity of sound is calculated and compared with the known velocity of sound for that layer. If these values agree, the selected T_j defines the true position of sound emittance. If they do not agree, an iteration process is carried out, until agreement is achieved within error limitations.

With the correct value for P_x, P_y, V_x, and V_y the horizontal wind components can then be found from equations (18b) and (18c).

V. COMPUTER SOLUTION

The solution for winds has been programmed for the IBM 7090 computer. Figure 5 shows the flow diagram for the wind solution.

The speed of sound profile is obtained from radiosonde and rocketsonde data, and above the altitude of these measurements, from "standard atmosphere" values. For the computer input the profile is piecewise linearized using 22 straight line segments.

The vehicle position data is entered at intervals of 0.5 seconds. Linear interpolation between these intervals agrees within 1 meter of the position determined from Lagrange's formula or Aitkin's method of iterative linear interpolation even at the highest vehicle speeds.

To insure convergence of the iterative process, ε_1 (the value within which V_j' and V_{avgj} are matched) and ε_2 (increment in T) must be compatible (Fig. 6). Counter parameters L and M assure that the solution has converged and indicate the direction of modification of the initial assumption of δT.

The relation between ε_1 and ε_2 is found as follows:

For the j^{th} noise event:

$$P_x = \frac{x_j - \sum_{k=1}^{j-1} \Delta x_k}{\tau - \sum_{k=1}^{j-1} \Delta t_k - T} \tag{21a}$$

$$P_y = \frac{y_j - \sum_{k=1}^{j-1} \Delta y_k}{\tau - \sum_{k=1}^{j-1} \Delta t_k - T} \tag{21b}$$

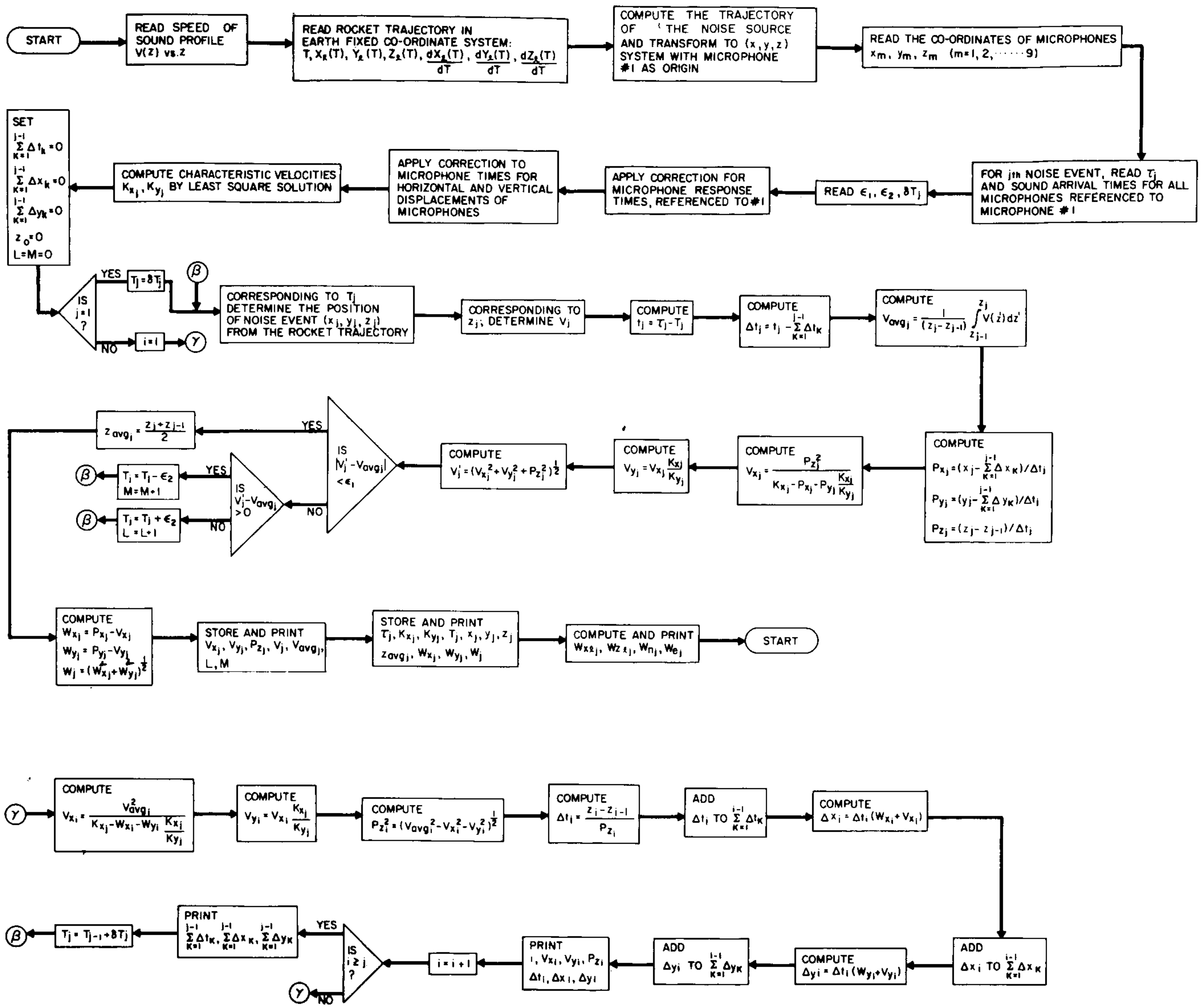

Fig. 5 FLOW DIAGRAM FOR WIND COMPUTATION

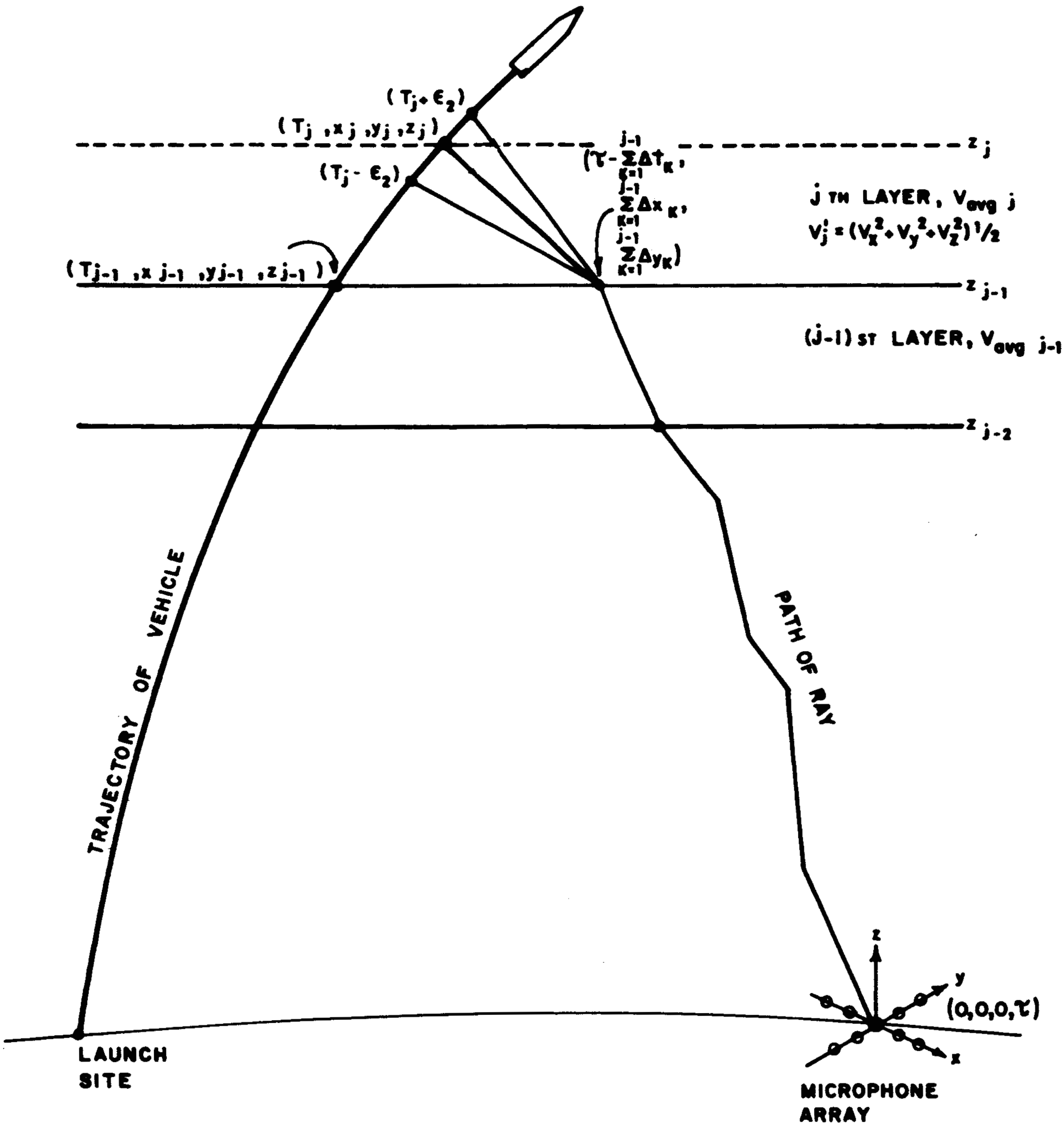

CONVERGENCE OF THE SOLUTION FOR DETERMINATION OF TIME AND POSITION OF THE j TH NOISE EVENT

THE CONDITION $|V_j' - V_{avg\,j}| \leq \epsilon_1$, DETERMINES THE POINT (T_j, x_j, y_j, z_j)

Fig. 6

and

$$P_z = \frac{z_j - z_{j-1}}{\tau - \sum_{k=1}^{j-1} \Delta t_k - T} \tag{21c}$$

Now

$$\frac{dP_x}{dT} = \frac{x_j - \sum_{k=1}^{j-1} \Delta x_k + (\tau - \sum_{k=1}^{j-1} \Delta t_k - T) \frac{dx}{dT}}{(\tau - \sum_{k=1}^{j-1} \Delta t_k - T)^2} \tag{22a}$$

$$\frac{dP_y}{dT} = \frac{y_j - \sum_{k=1}^{j-1} \Delta y_k + (\tau - \sum_{k=1}^{j-1} \Delta t_k - T) \frac{dy}{dT}}{(\tau - \sum_{k=1}^{j-1} \Delta t_k - T)^2} \tag{22b}$$

$$\frac{dP_z}{dT} = \frac{z_j - z_{j-1} + (\tau - \sum_{k=1}^{j-1} \Delta t_k - T) \frac{dz}{dT}}{(\tau - \sum_{k=1}^{j-1} \Delta t_k - T)^2} \tag{22c}$$

To simplify the computations it is assumed that the velocity of sound in the upper layer is constant and wind is sufficiently small so that the approximation $P_x \approx V_x$ and $P_y \approx V_y$ is justified. So

$$\left|\frac{dV}{dT}\right| \approx \left|\frac{dP}{dT}\right| = \left\{ \left(\frac{dP_x}{dT}\right)^2 + \left(\frac{dP_y}{dT}\right)^2 + \left(\frac{dP_z}{dT}\right)^2 \right\}^{1/2} \tag{23}$$

$$\varepsilon_1 = \left|\frac{dV}{dT}\right| \varepsilon_2 \tag{24}$$

Taking the case of j = 27 as an example,

$\tau = 310.0$ sec. $\qquad \frac{dx}{dT} = 1041.46$ m/s

$$\sum_{k=1}^{j-1} \Delta t_k = 182.4245 \text{ sec.} \qquad \frac{dy}{dT} = 422.09 \text{ m/s}$$

$$T = 120.8481 \text{ sec.} \qquad \frac{dz}{dT} = 1118.31 \text{ m/s}$$

$$x_j = 21878.1 \text{ m.} \qquad y_j = 16940.9 \text{ m.} \qquad z_j = 49280.7 \text{ m.}$$

$$\sum_{k=1}^{j-1} \Delta x_k = 21147.4 \qquad \sum_{k=1}^{j-1} \Delta y_k = 16452.6 \qquad z_{j-1} = 47423.4 \text{ m.}$$

these values give

$$\varepsilon_1 = 280\ \varepsilon_2$$

Based on an evaluation of overall system parameters, a criterion of 0.2 meters/sec. has been established as the value for ε_1 and equation (25) is used to determine the appropriate tolerance for ε_2.

VI. THE WIND PROFILE

Figures 7 and 8 graph the wind profile determined during the flight of the SA-9. Also plotted are the rocketsonde and rawinsonde measurements taken near the time of the SA-9 flight. The agreement between the methods is consistent with the results of the error analysis.

Table 1 lists the input quantities in the first four columns. The time and coordinates of the trajectory to which the solutions converged are listed under T_j (Range Zero = 14.37:00Z) x_j, y_j, and z_j. The remaining columns list the wind values in three coordinate systems: (1) the system of the microphone array (2) the system of the trajectory, and (3) the North-South, East-West system. The data points were computed at intervals of 10 seconds τ.

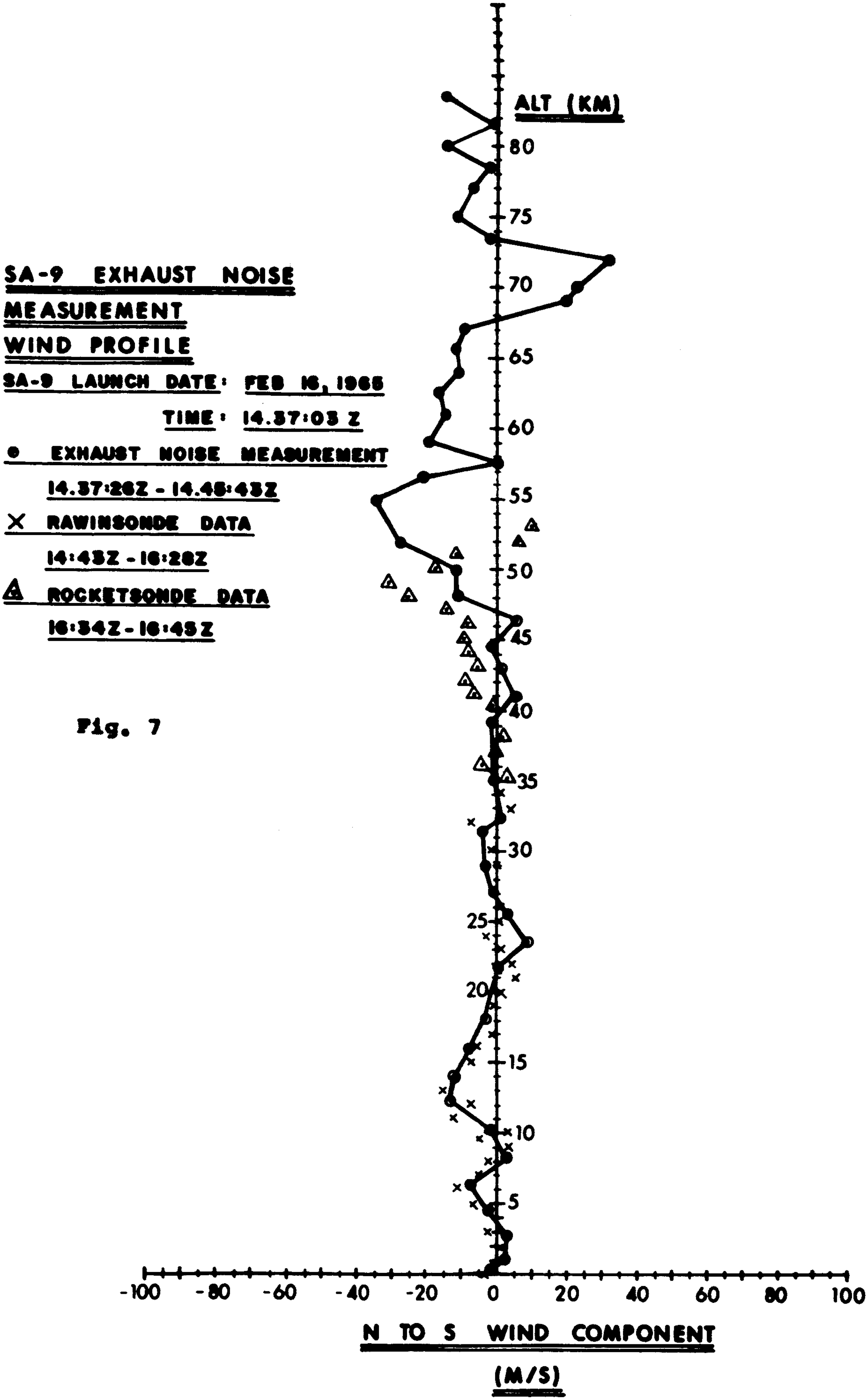

ALT (KM)
80
75
70
65
60
55
50
45
40
35
30
25
20
15
10
5
SA-9 EXHAUST NOISE
MEASUREMENT
WIND PROFILE
SA-9 LAUNCH DATE: FEB 16, 1965
TIME: 14.37:03 Z
EXHAUST NOISE MEASUREMENT
14.37:26Z - 14.45:43Z
RAWINSONDE DATA
14:43Z - 16:28Z
ROCKETSONDE DATA
16:34Z - 16:45Z
-100
-80
-60
-40
-20
0
20
40
60
80
100
N TO S WIND COMPONENT
(M/S)

Fig. 7

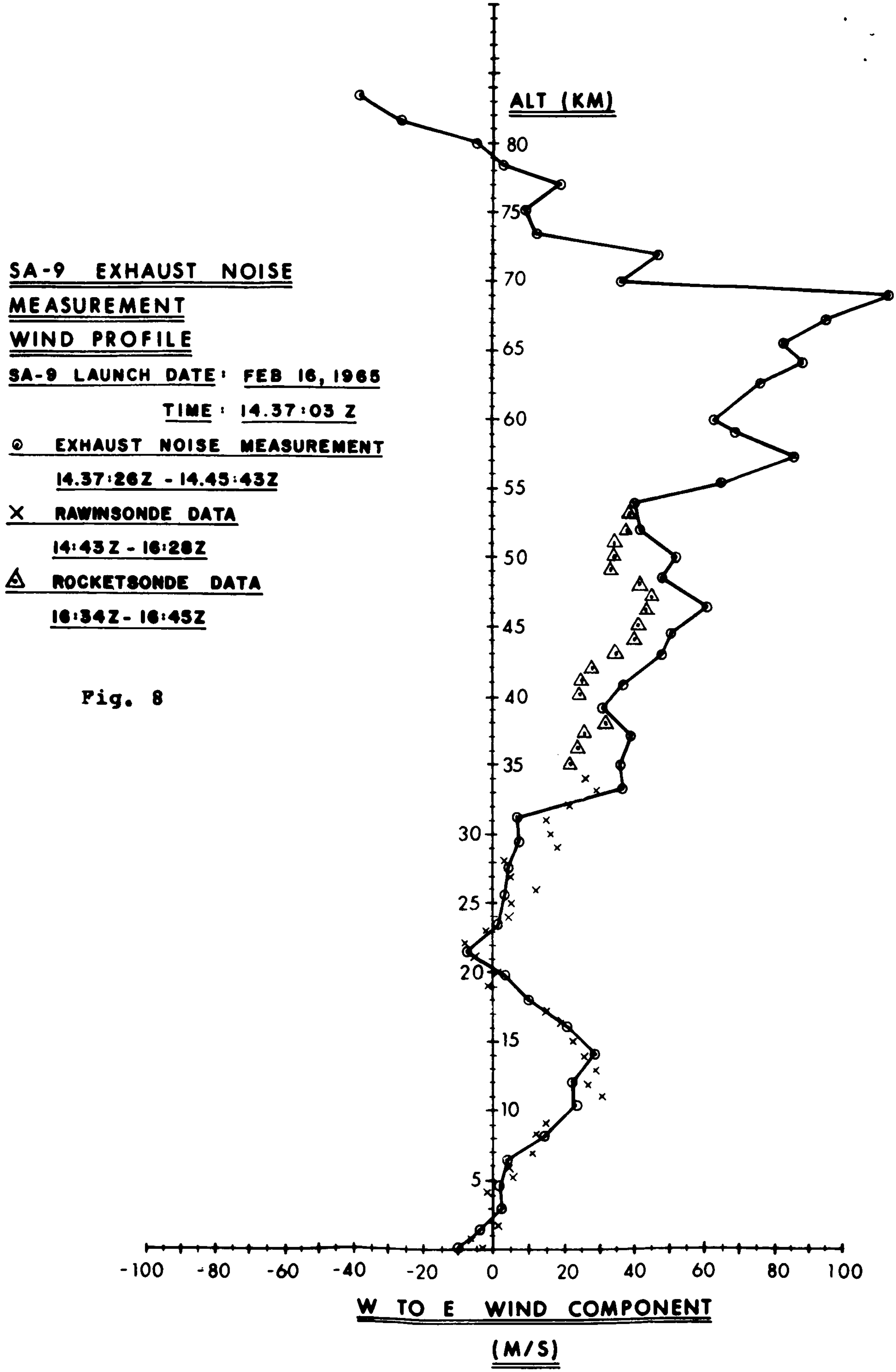
SA-9 EXHAUST NOISE MEASUREMENT WIND PROFILE
SA-9 LAUNCH DATE: FEB 16, 1965
TIME: 14.37:03 Z
EXHAUST NOISE MEASUREMENT
14.37:26Z - 14.45:43Z
RAWINSONDE DATA
14:43Z - 16:28Z
ROCKETSONDE DATA
16:34Z - 16:45Z
ALT (KM)
80
75
70
65
60
55
50
45
40
35
30
25
20
15
10
5
-100
-80
-60
-40
-20
0
20
40
60
80
100
W TO E WIND COMPONENT
(M/S)

Fig. 8

J	TAU SEC	KX M/S	KY M/S	T SEC	X METERS	Y METERS	Z METERS	ZAVG METERS	WX M/S	WY M/S	WXL M/S	WZL M/S	WN M/S	WE M/S
1	50.00	399.361	-651.696	24.0539	-7340.5	4766.8	871.3	435.6	-9.00	-4.83	-10.2	1.1	1.6	-10.1
2	60.00	412.678	-651.740	33.6927	-7271.5	4793.3	2015.5	1443.4	-2.12	-3.51	-3.3	2.5	-1.5	-3.8
3	70.00	446.360	-654.368	42.6771	-7029.7	4892.3	3593.0	2804.3	3.95	-1.24	3.2	2.6	-3.4	2.4
4	80.00	503.751	-664.680	50.4690	-6614.2	5064.0	5411.9	4502.4	-.16	2.37	.7	-2.3	2.0	1.3
5	90.00	595.671	-680.373	57.1450	-6071.5	5301.6	7336.3	6374.1	-.82	7.49	2.0	-7.3	6.5	3.9
6	100.00	749.997	-703.672	63.0445	-5411.7	5589.3	9315.2	8325.8	13.94	6.21	15.3	-.5	-3.4	14.9
7	110.00	988.429	-721.932	68.1878	-4668.9	5909.0	11263.3	10289.3	17.36	15.06	21.7	-7.5	1.6	22.9
8	120.00	1352.509	-732.422	72.6964	-3867.4	6263.1	13163.8	12213.6	10.48	24.72	19.0	-19.0	13.4	23.2
9	130.00	2018.866	-739.287	76.7159	-3016.6	6641.9	15026.3	14095.1	15.85	26.53	24.6	-18.7	11.6	28.6
10	140.00	3531.482	-750.593	80.3849	-2108.7	7041.7	16876.4	15951.4	12.64	18.35	18.6	-12.3	7.0	21.1
11	150.00	9973.709	-767.034	83.7945	-1139.2	7462.5	18734.4	17805.4	5.93	9.37	9.0	-6.5	3.9	10.4
12	160.00	-15921.402	-788.305	87.0341	-93.0	7910.4	20631.3	19682.8	2.01	2.53	2.8	-1.6	.8	3.1
13	170.00	-4893.866	-815.274	90.1443	1040.7	8390.1	22579.5	21605.4	-6.51	-5.86	-8.2	3.0	-.8	-8.7
14	180.00	-2906.231	-841.160	93.0844	2239.8	8893.2	24539.1	23559.3	6.85	-6.81	3.8	8.9	-9.6	1.4
15	190.00	-2140.038	-861.576	95.8604	3496.6	9417.5	26497.7	25518.4	4.25	-1.17	3.5	2.7	-3.5	2.7
16	200.00	-1733.195	-876.660	98.4837	4806.5	9963.4	28441.9	27469.8	2.18	3.33	3.3	-2.3	1.3	3.7
17	210.00	-1475.187	-888.456	100.9837	6171.3	10528.8	30387.7	29414.8	4.36	7.22	6.7	-5.1	3.1	7.8
18	220.00	-1301.153	-898.791	103.3697	7585.9	11111.9	32331.8	31359.8	2.75	7.49	5.4	-5.9	4.3	6.7
19	230.00	-1154.535	-901.329	105.6036	9015.1	11699.3	34227.8	33279.8	30.67	20.82	36.2	-7.8	-1.8	37.0
20	240.00	-1048.201	-902.960	107.7538	10492.1	12305.0	36123.9	35175.9	28.75	22.52	35.1	-10.1	.7	36.5
21	250.00	-965.721	-903.942	109.8247	12012.1	12926.9	38017.1	37070.5	31.56	24.18	38.3	-10.6	.3	39.8
22	260.00	-903.289	-906.961	111.8477	13593.2	13572.7	39931.8	38974.5	24.77	20.01	30.5	-9.3	1.1	31.8
23	270.00	-850.222	-910.599	113.7947	15208.3	14231.2	41837.2	40884.5	32.75	17.84	37.0	-4.3	-5.5	36.9
24	280.00	-805.303	-910.123	115.6550	16840.0	14895.3	43716.5	42776.9	39.39	28.05	47.0	-11.2	-1.3	48.3
25	290.00	-767.938	-908.374	117.4494	18498.3	15569.5	45584.9	44650.7	39.99	31.76	49.0	-14.5	1.3	51.1
26	300.00	-734.054	-906.412	119.1639	20163.8	16245.7	47423.4	46504.2	52.35	32.40	60.7	-10.4	-5.6	61.3
27	310.00	-708.860	-902.945	120.8481	21878.1	16940.9	49280.7	48352.0	31.68	37.55	43.4	-22.9	10.9	47.9
28	320.00	-686.617	-898.718	122.4709	23605.0	17640.5	51119.8	50200.2	34.01	40.50	46.7	-24.8	11.9	51.5
29	330.00	-669.506	-892.483	124.0535	25363.5	18352.1	52962.2	52041.0	17.41	47.51	33.9	-37.5	27.5	42.5
30	340.00	-655.064	-885.162	125.5856	27137.3	19069.0	54793.1	53877.7	11.03	52.02	29.7	-44.1	34.9	40.1
31	350.00	-638.614	-877.417	127.0187	28860.6	19764.9	56548.5	55670.8	39.07	55.45	57.0	-36.8	20.8	64.6
32	360.00	-620.848	-871.198	128.3649	30539.1	20442.1	58236.9	57392.7	69.15	51.31	83.3	-21.7	-.6	86.1
33	370.00	-607.293	-863.655	129.6932	32251.9	21132.7	59941.1	59089.0	43.11	57.11	61.4	-36.8	19.7	68.8
34	380.00	-595.009	-857.844	130.9856	33972.9	21826.1	61635.6	60788.3	41.64	49.75	57.2	-30.5	14.7	63.2
35	390.00	-583.196	-850.393	132.2139	35662.3	22506.4	63282.4	62459.0	50.16	59.55	68.8	-36.4	17.4	75.9
36	400.00	-571.441	-843.044	133.3821	37316.1	23171.9	64880.4	64081.4	64.26	61.77	82.7	-33.2	10.7	88.5
37	410.00	-561.000	-836.270	134.5225	38976.6	23839.6	66471.7	65676.1	58.59	59.75	76.7	-33.4	12.5	82.7
38	420.00	-550.751	-829.120	135.6070	40600.2	24492.2	68015.0	67243.3	70.63	64.95	89.8	-33.8	9.4	95.5
39	430.00	-539.671	-824.547	136.6314	42173.1	25124.0	69499.4	68757.2	102.36	52.62	114.6	-10.4	-19.6	113.4
40	440.00	-531.907	-827.416	137.7362	43914.0	25822.9	71130.2	70314.8	43.10	3.58	41.3	12.8	-23.1	36.6
41	450.00	-523.882	-830.045	138.7898	45617.9	26506.4	72714.5	71922.4	57.12	2.74	54.0	18.9	-32.2	47.3
42	460.00	-519.086	-831.415	139.8757	47419.9	27228.9	74377.6	73546.0	8.77	9.33	11.6	-5.4	2.2	12.6
43	470.00	-515.010	-831.464	140.9367	49226.5	27952.9	76032.7	75205.1	.23	15.01	5.8	-13.8	11.8	9.2
44	480.00	-510.463	-830.989	141.9483	50998.0	28662.4	77643.9	76838.3	10.87	16.83	16.4	-11.5	6.9	18.8
45	490.00	-506.611	-832.588	142.9602	52808.6	29387.4	79279.4	78461.6	.44	3.43	1.7	-3.0	2.5	2.4
46	500.00	-503.674	-833.101	143.9613	54641.3	30120.8	80923.9	80101.6	-13.39	8.29	-9.3	-12.7	14.7	-5.7
47	510.00	-501.319	-837.799	144.9798	56532.3	30877.5	82610.7	81767.3	-22.28	-15.49	-26.5	6.0	1.0	-27.1
48	520.00	-500.249	-841.668	146.0120	58472.5	31653.5	84331.1	83470.9	-40.88	-11.04	-42.0	-5.1	15.8	-39.3

SATURN SA-9 WIND RESULTS

Table 1

VII. ERROR ANALYSIS

Four sources of errors are considered in this analysis.

1) Error in the measurement of sound arrival times at each microphone. This introduces error in the derived value of characteristic velocity K_x, K_y.
2) Error in the speed of sound profile.
3) Uncertainty in the position of the noise source with respect to the vehicle.
4) Error from plane wave assumption.

7.1 Sound Arrival Time Error

It will be shown that error in characteristic velocity determination is the most significant contributor to wind error. The errors in the j^{th} layer winds due to a characteristic velocity error arise from two distinct sources. First, an implicit error is introduced in the winds because the result of the ray tracing to the top surface of the $(j-1)^{st}$ layer is displaced from the actual point of penetration. Second, wind error is introduced explicitly in the j^{th} layer from the error in K_{x_j}, K_{y_j}.

Both types of error can be studied from a consideration of Fig. 9. The following equations are derived from inspection of this figure.

$$\left\{ \sum_{k=1}^{j-1} \Delta x_k - x_j - W_x\left(\tau_j - T_j - \sum_{k=1}^{j-1} \Delta t_k\right) \right\}^2 + \left\{ \sum_{k=1}^{j-1} \Delta y_k - y_j - W_y\left(\tau_j - T_j - \sum_{k=1}^{j-1} \Delta t_k\right) \right\}^2 + (z_{j-1} - z_j)^2 = V_{avgj}^2 \left(\tau_j - T_j - \sum_{k=1}^{j-1} \Delta t_k\right)^2 \quad (26)$$

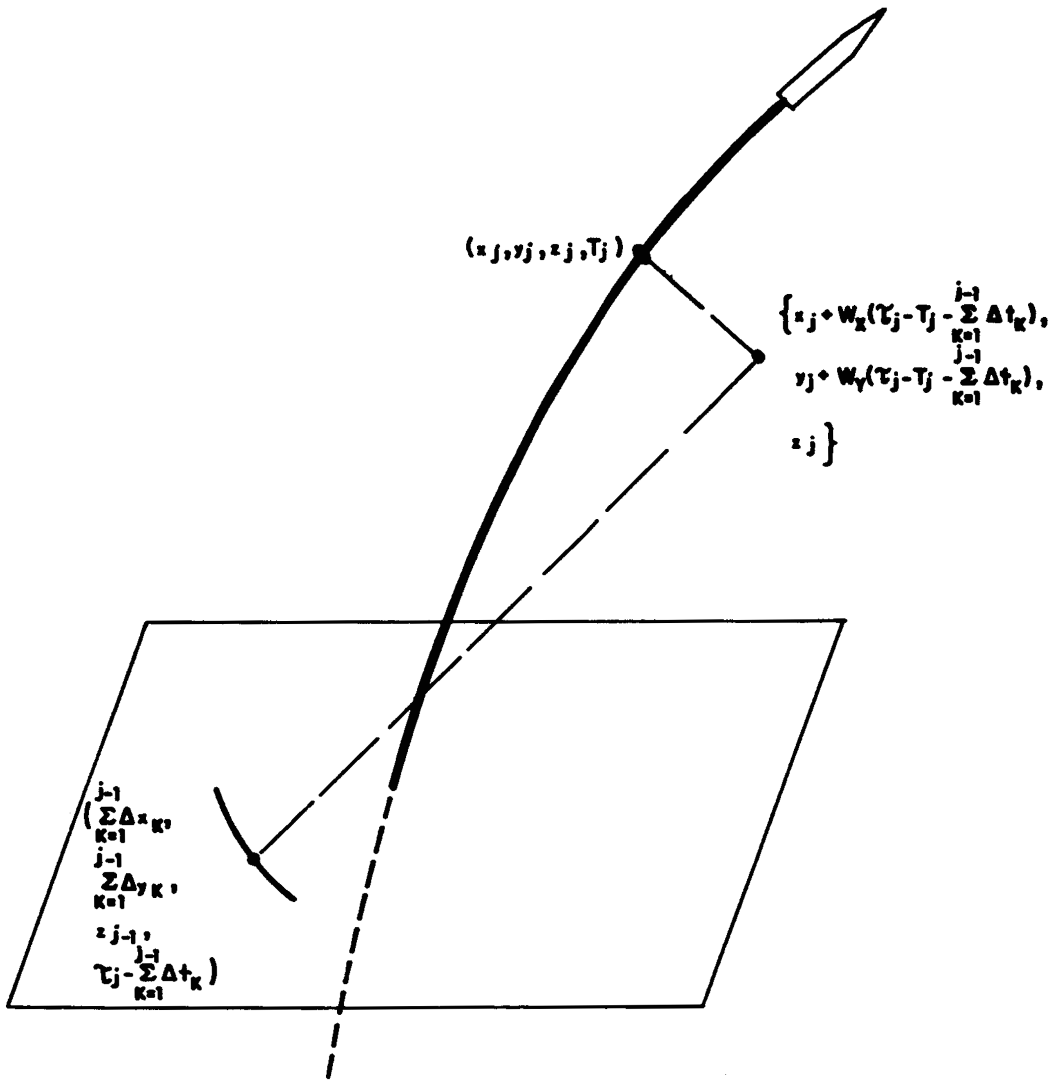

THE ARRIVAL OF THE jTH NOISE EVENT AT

$$\left(\sum_{K=1}^{j-1} \Delta x_K , \sum_{K=1}^{j-1} \Delta y_K , z_{j-1} \right)$$

Fig. 9

This is simply the expression of an expanding spherical wave in a moving medium.

The direction cosines of the ray at $\left(\sum_{k=1}^{j-1} \Delta x_k, \sum_{k=1}^{j-1} \Delta y_k, z_{j-1} \right)$ are

$$\alpha = \frac{x_j + W_x \Delta t_j - \sum_{k=1}^{j-1} \Delta x_k}{V_{avgj} \Delta t_j} \tag{27a}$$

$$\beta = \frac{y_j + W_y \Delta t_j - \sum_{k=1}^{j-1} \Delta y_k}{V_{avgj} \Delta t_j} \tag{27b}$$

$$\gamma = \frac{z_j - z_{j-1}}{V_{avgj} \Delta t_j} \tag{27c}$$

where $\Delta t_j = \tau_j - T_j - \sum_{k=1}^{j-1} \Delta t_k$

The characteristic velocities are then

$$K_x = - \frac{V_{avgj}}{\alpha} + W_x + W_y \ \beta/\alpha \tag{28a}$$

$$K_y = - \frac{V_{avgj}}{\beta} + W_y + W_x \ \alpha/\beta \tag{28b}$$

For simplicity in writing let

$V = V_{avgj}$; $x_o = \sum_{k=1}^{j-1} \Delta x_k$ etc. ; $t_o = \sum_{k=1}^{j-1} \Delta t_k$

Keeping in mind that the trajectory gives

$$\begin{aligned} x_j &= x_j \ (T) \\ y_j &= y_j \ (T) \\ z_j &= z_j \ (T) \end{aligned} \tag{29}$$

and that $\Delta t_j = \tau_j - T_j - t_o$

the above equations can be rearranged to give

$$F(K_x,K_y,W_x,W_y,T_j,t_o,x_o,y_o,V) = (K_x-W_x)(x_j-W_x\Delta t_j-x_o)+V^2\Delta t_j-W_y(y_j+W_y\Delta t_j-y_o) = 0 \qquad (30)$$

$$G(K_x,K_y,W_x,W_y,T_j,t_o,x_o,y_o,V) = (K_y-W_y)(y_j-W_y\Delta t_j-y_o)+V^2\Delta t_j-W_x(x_j+W_x\Delta t_j-x_o) = 0 \qquad (31)$$

$$H(K_x,K_y,W_x,W_y,T_j,t_o,x_o,y_o,V) = (x_j+W_x\Delta t_j-x_o)^2+(y_j+W_y\Delta t_j-y_o)^2+(z_j-z_o)^2-V^2\Delta t_j^2 = 0 \qquad (32)$$

Treating W_x, W_y and T as dependent variables the Jacobian of this system of equations is

$$J = \frac{\partial(F,G,H)}{\partial(W_x,W_y,T)} = \begin{vmatrix} F_{W_x} & F_{W_y} & F_T \\ G_{W_x} & G_{W_y} & G_T \\ H_{W_x} & H_{W_y} & H_T \end{vmatrix} \qquad (33)$$

where $\frac{\partial F}{\partial W_x}$ is denoted by F_{W_x} etc.

Then

$$\frac{\partial W_x}{\partial K_x} = -\frac{\begin{vmatrix} F_{K_x} & F_{W_y} & F_T \\ G_{K_x} & G_{W_y} & G_T \\ H_{K_x} & H_{W_y} & H_T \end{vmatrix}}{J} \qquad (34)$$

$$\frac{\partial W_x}{\partial x_o} = -\frac{\begin{vmatrix} F_{x_o} & F_{W_y} & F_T \\ G_{x_o} & G_{W_y} & G_T \\ H_{x_o} & H_{W_y} & H_T \end{vmatrix}}{J} \qquad \frac{\partial W_x}{\partial t_o} = -\frac{\begin{vmatrix} F_{t_o} & F_{W_y} & F_T \\ G_{t_o} & G_{W_y} & G_T \\ H_{t_o} & H_{W_y} & H_T \end{vmatrix}}{J} \qquad (35)$$

and similarly for $\frac{\partial W_x}{\partial K_y}$, $\frac{\partial W_x}{\partial y_o}$, $\frac{\partial W_y}{\partial K_x}$, $\frac{\partial W_y}{\partial K_y}$, $\frac{\partial W_y}{\partial x_o}$, $\frac{\partial W_y}{\partial y_o}$, and $\frac{\partial W_y}{\partial t_o}$

The partial derivatives of W with respect to x_o, y_o, and t_o give an indication of the first type of error, mentioned earlier. The derivatives of W with respect to characteristic velocity are a measure of the second type.

The total error in j^{th} layer winds due to an error in the j^{th} characteristic velocities is:

$$\Delta W_{x_j} = \left(\frac{\partial W_x}{\partial K_x}\right)_j \Delta K_{x_j} + \left(\frac{\partial W_x}{\partial K_y}\right)_j \Delta K_{y_j} + \left(\frac{\partial W_x}{\partial x_o}\right)_j \Delta x_o + \left(\frac{\partial W_x}{\partial y_o}\right)_j \Delta y_o + \left(\frac{\partial W_x}{\partial t_o}\right)_j \Delta t_o \quad (3$$

A similiar expression can be written for ΔW_{y_j}.

In order to evaluate ΔW_{x_j} it is necessary to evaluate Δt_o, Δx_o and Δy_o. These parameters are computed by ray tracing each value of K_x and K_y to the level z_{j-1}. The error in the characteristic velocities can be related to errors in the measured time of arrival at the m^{th} microphone by

$$\Delta K_x = - \Delta A_{x_m} \frac{K_x^2}{x_m} \quad (37a)$$

$$\Delta K_y = - \Delta A_{y_m} \frac{K_y^2}{y_m} \quad (37b)$$

Calculated values of ΔW_x and ΔW_y are shown in Fig. 10 and 11 and are listed in Table 2 along with actual differences from wind computations for errors of .5 ms and 2 ms. These computations were made for τ = 100,150,200,250 etc. These time of arrival errors are introduced into every microphone pair and in the same direction to maximize the resultant wind error.

An interesting observation from Table 2 is that the errors in the j^{th} layer winds caused by errors introduced into the characteristic velocity for that layer, result in a nearly equal

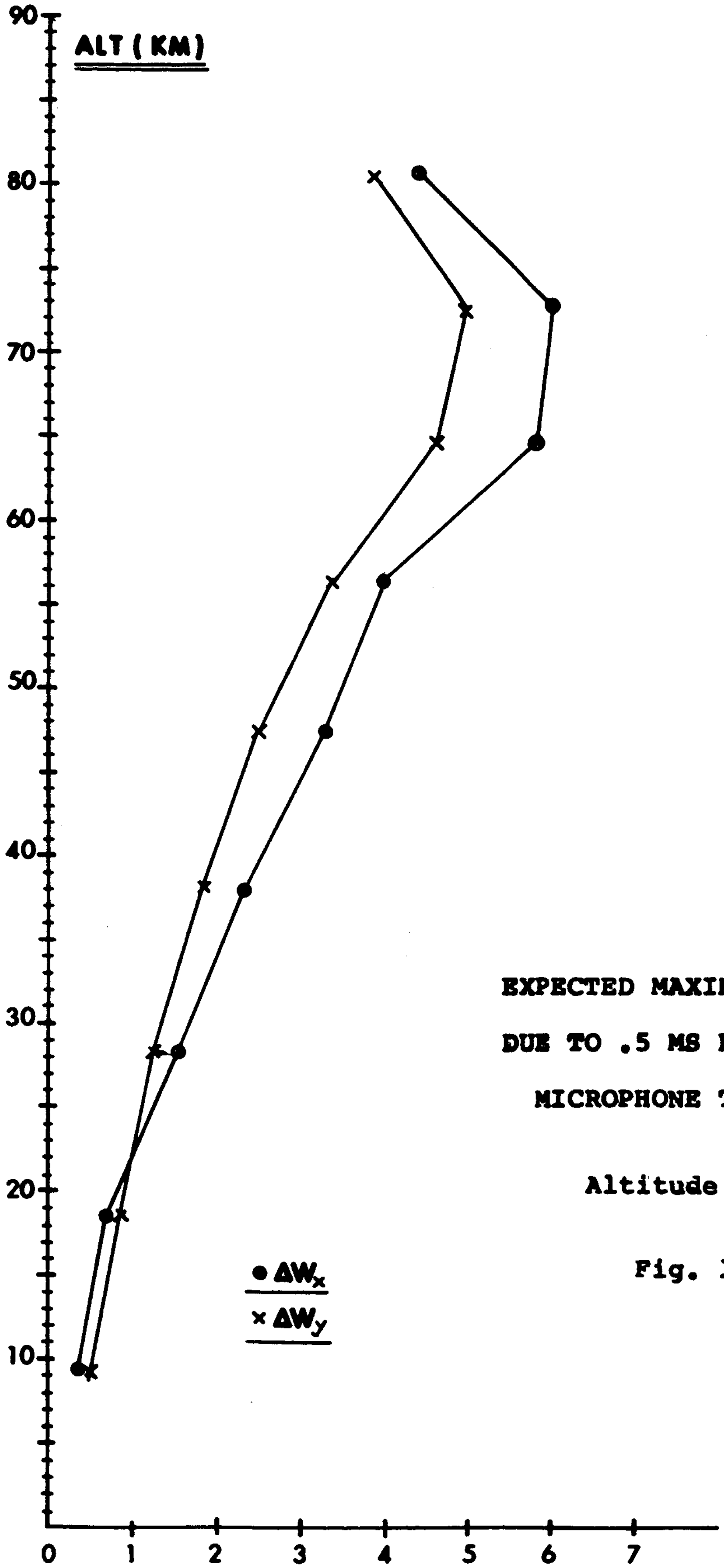

EXPECTED MAXIMUM WIND ERROR DUE TO .5 MS ERROR IN ALL MICROPHONE TIMES

Altitude vs. ΔW_x, ΔW_y

Fig. 10

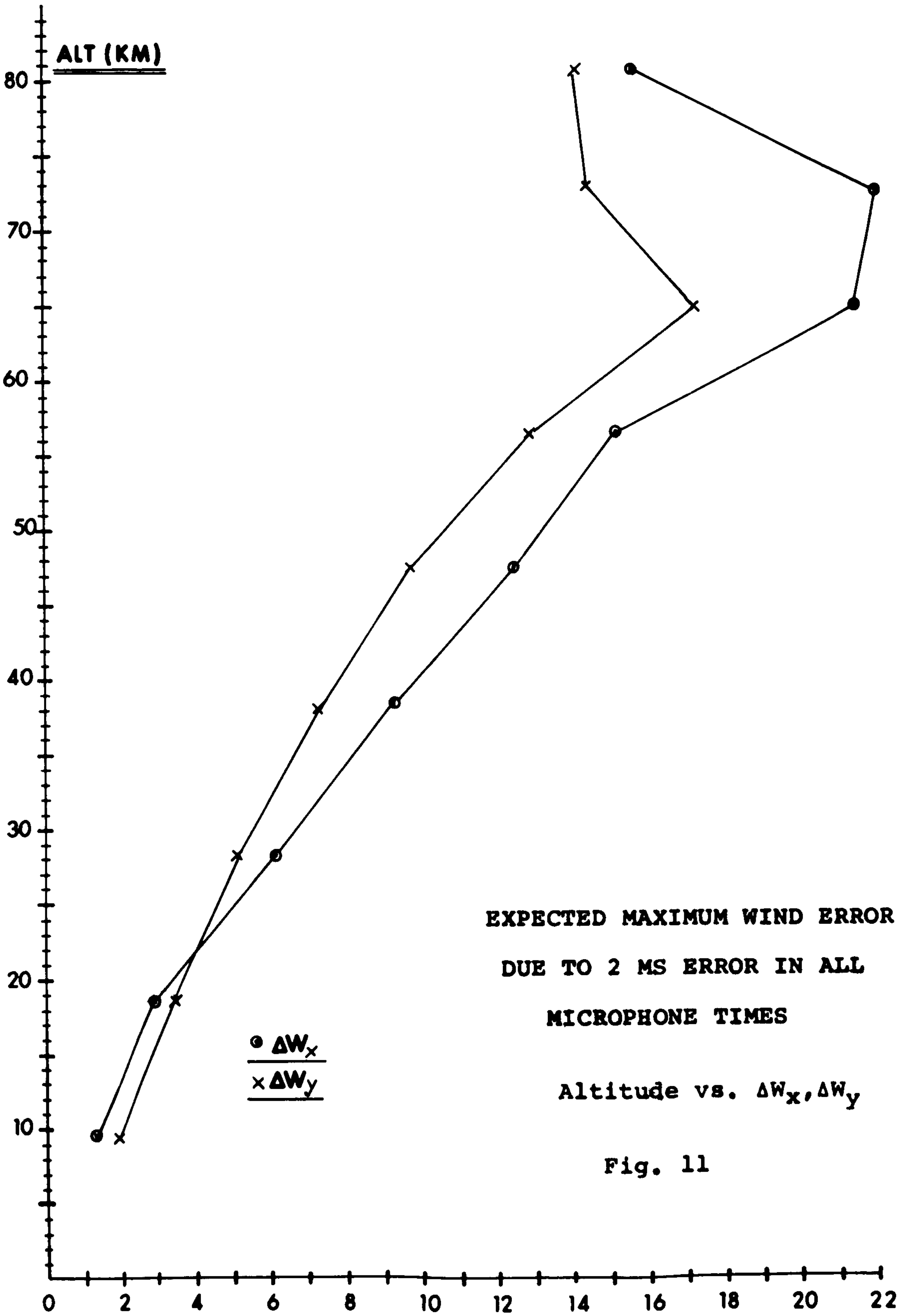

EXPECTED MAXIMUM WIND ERROR
DUE TO 2 MS ERROR IN ALL
MICROPHONE TIMES

Altitude vs. $\Delta W_x, \Delta W_y$

Fig. 11

WIND MEASUREMENT--ERROR ANALYSIS (SA-9)

		ERRORS DUE TO .5 MS.				ERRORS DUE TO 2. MS.			
		COMPUTED		ACTUAL		COMPUTED		ACTUAL	
TAU	ALT	DWX	DWY	DWX	DWY	DWX	DWY	DWX	DWY
SEC	METERS	M/S	M/S	M/S	M/S	M/S	M/S	M/S	M/S
50	436	.00	.00	-.00	-.00	.00	.00	-.00	-.00
60	1443	.00	.00	-.00	-.00	.00	.00	-.00	-.00
70	2804	.00	.00	.00	-.00	.00	.00	.00	-.00
80	4502	.00	.00	-.00	.00	.00	.00	-.00	.00
90	6374	.00	.00	-.00	.00	.00	.00	-.00	.00
100	8326	-.33	.48	-.32	.48	-1.31	1.93	-1.32	1.93
110	10289	.30	-.56	.33	-.51	1.25	-2.28	1.55	-2.25
120	12214	-.01	.01	-.01	.01	-.25	.18	-.23	.22
130	14095	-.01	.01	-.00	.00	.00	.01	.01	-.00
140	15951	-.00	.00	-.00	.00	-.01	.02	-.01	.01
150	17805	-.71	.86	-.71	.87	-2.84	3.46	-2.82	3.44
160	19683	.62	-.90	.80	-.98	2.47	-3.57	2.94	-3.54
170	21605	-.16	.10	-.10	.16	-.19	.11	-.10	.16
180	23559	.02	-.01	.01	-.02	.00	-.00	-.00	.00
190	25518	-.00	.00	-.00	.00	.00	-.00	-.00	.00
200	27470	1.57	1.28	1.56	1.28	6.28	5.10	6.22	5.05
210	29415	-1.82	-1.40	-1.59	-1.30	-7.32	-5.60	-6.39	-5.37
220	31360	-.00	.00	-.00	-.00	-.13	.09	-.02	.04
230	33280	-.00	.00	-.00	-.00	-.11	.06	-.03	.09
240	35176	-.00	.00	-.00	-.00	-.01	-.00	-.01	-.01
250	37071	2.37	1.87	2.35	1.85	9.46	7.48	9.28	7.32
260	38975	-2.79	-2.00	-2.34	-1.91	-11.15	-8.02	-9.45	-7.53
270	40885	-.04	.06	.04	.10	-.04	.06	.02	.09
280	42777	.00	-.01	.01	.00	.00	-.01	-.01	-.01
290	44651	-.00	-.01	-.02	-.03	.00	-.00	-.01	-.01
300	46504	3.24	2.54	3.24	2.52	12.98	10.07	12.52	9.74
310	48352	-3.76	-2.74	-3.01	-2.50	-14.99	-11.00	-12.56	-10.43
320	50200	-.01	-.00	.02	.01	.03	.07	.05	.06
330	52041	-.02	-.00	.01	.01	.04	.01	.03	.02
340	53878	-.02	-.01	.01	.01	.04	-.02	-.01	-.02
350	55671	4.00	3.40	3.99	3.38	16.09	13.60	15.21	12.96
360	57393	-5.96	-4.08	-4.85	-3.71	-23.72	-16.30	-20.60	-15.67
370	59089	.03	.00	-.01	-.01	.37	.07	-.19	-.11
380	60788	.03	.00	-.01	-.01	.42	.09	-.18	-.10
390	62459	.03	.01	-.01	-.01	.46	.08	-.22	-.13
400	64081	5.97	4.69	5.79	4.58	24.18	18.80	21.54	17.22
410	65676	-7.38	-5.16	-5.97	-4.75	-29.05	-20.57	-25.90	-20.36
420	67243	.06	.03	.02	.03	.94	.19	-.46	-.29
430	68757	.07	-.00	-.03	-.02	.99	.28	-.56	-.29
440	70315	.07	.01	-.06	-.05	1.08	.38	-.22	-.08
450	71922	6.25	4.02	6.04	3.90	25.87	16.30	22.09	14.37
460	73546	-5.68	-3.99	-4.49	-3.64	-21.76	-15.67	-19.63	-15.66
470	75205	-.03	.01	.08	.06	1.07	.34	-.11	-.08
480	76838	-.06	-.04	.02	.00	1.14	.36	-.07	-.05
490	78462	-.06	-.04	.02	.01	1.09	.33	-.15	-.12
500	80102	4.30	3.84	4.36	3.87	18.59	15.87	15.71	14.20
510	81767	-5.03	-3.61	-4.00	-3.31	-18.61	-13.75	-17.09	-13.91
520	83471	-.09	-.01	.07	.05	1.07	.36	.01	.02

WIND ERRORS DUE TO .5 MS AND 2.0 MS ERRORS IN ALL MICROPHONE TIMES

Table 2

and opposite error in the $(j + 1)^{st}$ layer and practically no error thereafter. Thus, averaging 3 successive layers can reduce the percentage error approximately by a factor of 3. This however has the undesirable effect of decreasing resolution by 1/3.

This suggests the possibility of varying the initial layer thickness (thereby changing single layer errors) until both the resolution and the accuracy are optimized. Some effort was made along these lines but no significant gains were realized. In order to simultaneously improve accuracy and resolution of the result it is necessary to decrease the error in the input data.

Repeated reading of arrival times exhibit a scatter that indicate the uncertainty in the arrival times is between 2 and 2.5 ms. The system parameters were chosen on the basis of uncertainties of about half this value. This larger error is attributed to slight differences in microphone characteristics, differences in local background conditions, and to limitations in manual reading of this type of data presentation.

To the extent that these effects are random the errors can be reduced by using a computer programmed for cross correlation. In such a program the time difference between two channels is determined by an integration over a preset segment of the data rather than from a single wave form, thus reducing small random errors. Automatic cross correlation has not yet been used because of prohibitively high computer time requirements, but recently acquired equipment, and an improved programming method hold promise for this technique.

The use of higher frequencies of the noise spectrum also offers the possibility of increased precision in determining arrival time. Experimentation with wide band microphones is planned to evaluate this possibility.

7.2 Errors in the Speed of Sound Profile

The temperature up to 30 km is measured by radiosonde and an accuracy of $\pm$ 1°C is claimed for these data. Above 30 km the temperature data are estimated to be in error by a maximum of 10°C.

$\frac{\partial W_x}{\partial V} \Delta V$ and $\frac{\partial W_y}{\partial V} \Delta V$ for a single layer can be calculated readily by the analytical technique described above. However, to account for the speed of sound errors in lower layers a different approach must be followed.

A straight forward way of estimating these functions is to modify V(z) and compare the resulting winds. This was done as follows: Using the speed of sound profile as given in the trajectory a "standard" wind profile was determined. Then V(z) was replaced by

1) V(z) + 2 m/sec, for z > 30 km (2.7° - 3.3°C temperature error)

2) V(z) + 5 m/sec, for z > 30 km (6.8 - 8.3°C temperature error)

and new wind profiles were derived. These should represent a "worst case" analysis since a constant displacement gives largest errors in the integrated speed of sound. Fig. 12 shows ΔW_x and ΔW_y as a function of altitude for these two cases.

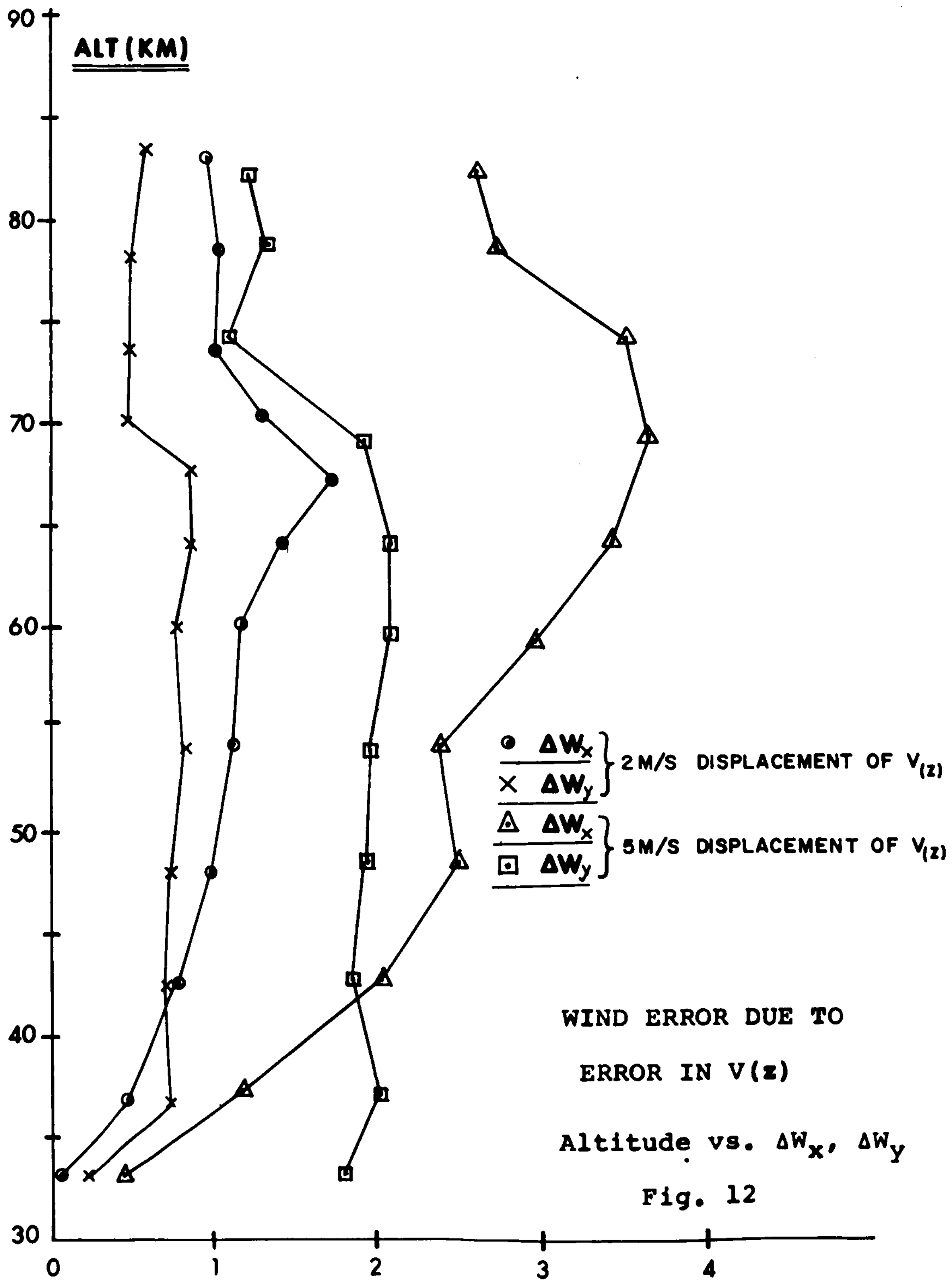

WIND ERROR DUE TO

ERROR IN V(z)

Altitude vs. ΔW_x, ΔW_y

Fig. 12

7.3 Noise Source Position Uncertainty

The mechanism of exhaust noise generation is fairly well understood, but there remains an uncertainty in the precise location of the noise source with respect to the vehicle. For the SA-9 data, the source was assumed to be on the trajectory 150 meters aft of the nozzle. To determine the sensitivity to an error in this estimate, the position of the source was displaced 100 meters and a new wind profile determined. Figure 13 shows the results of this displacement and indicates that this error is probably not significant.

7.4 Error from Plane Wave Assumption

The wave front deviates slightly from planar and to estimate the amount of error this induces, a spherical wave is considered.

Fig. 14 is a schematic of two microphones equally spaced about the origin of a coordinate system. A source of sound is located at (x', y', z') in this system. It is assumed that the temperature is constant throughout (Constant speed of sound, V) and that the winds are zero.

Since R is large compared with y_o a plane wave approximation at the array should be nearly correct. The time required for such a plane wave to cross the array is:

$$t_{-y_o} - t_{+y_o} = \frac{2y_o}{V}\frac{y'}{R} \tag{38}$$

The time interval for a spherical wave is

$$t_{-y_o} - t_{+y_o} = \frac{1}{V}\{[x'^2 + z'^2 + (y' + y_o)^2]^{\frac{1}{2}} - [x'^2 + z'^2 + (y' - y_o)^2]^{\frac{1}{2}}\} \tag{39}$$

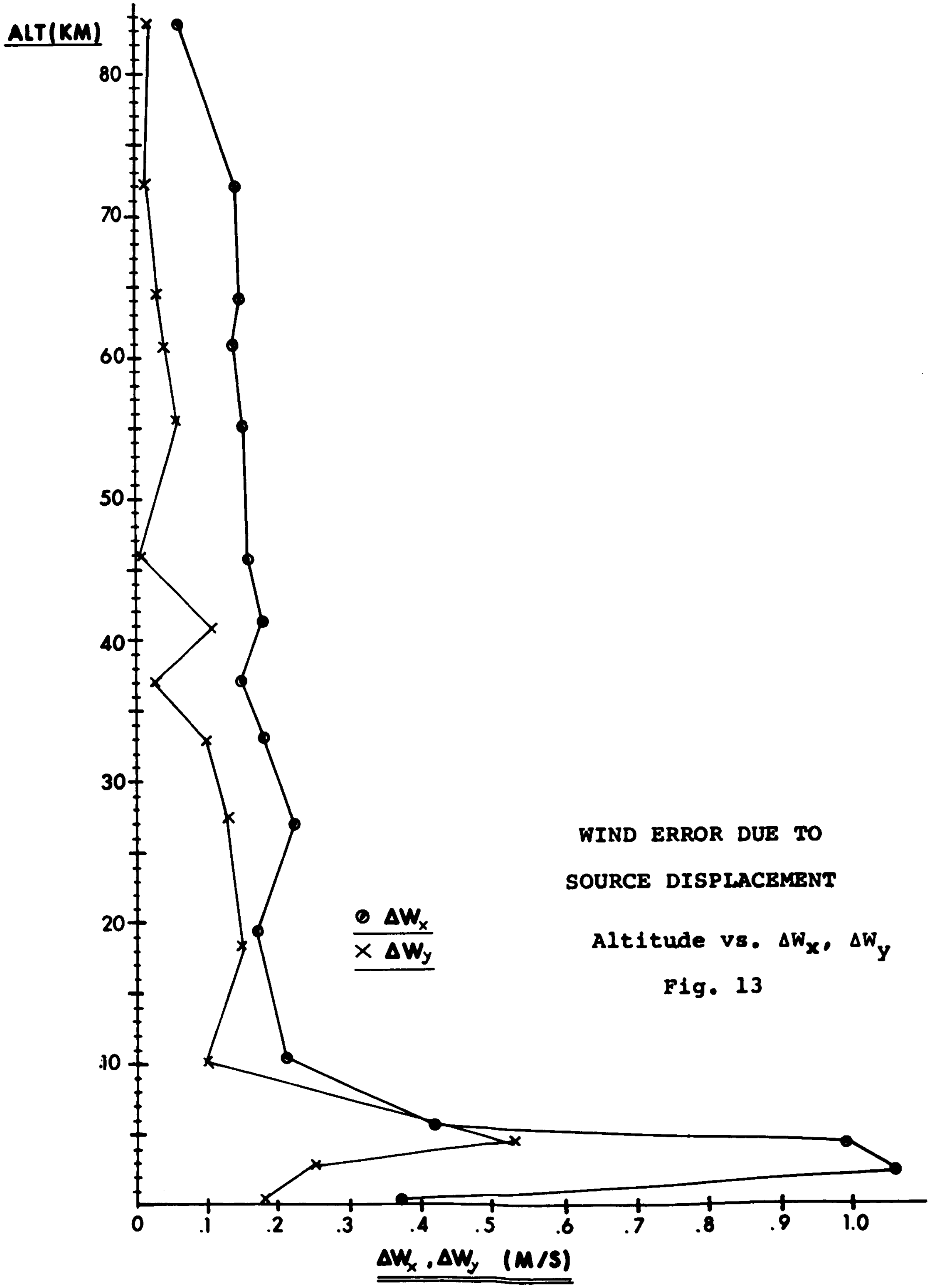

WIND ERROR DUE TO

SOURCE DISPLACEMENT

Altitude vs. ΔW_x, ΔW_y

Fig. 13

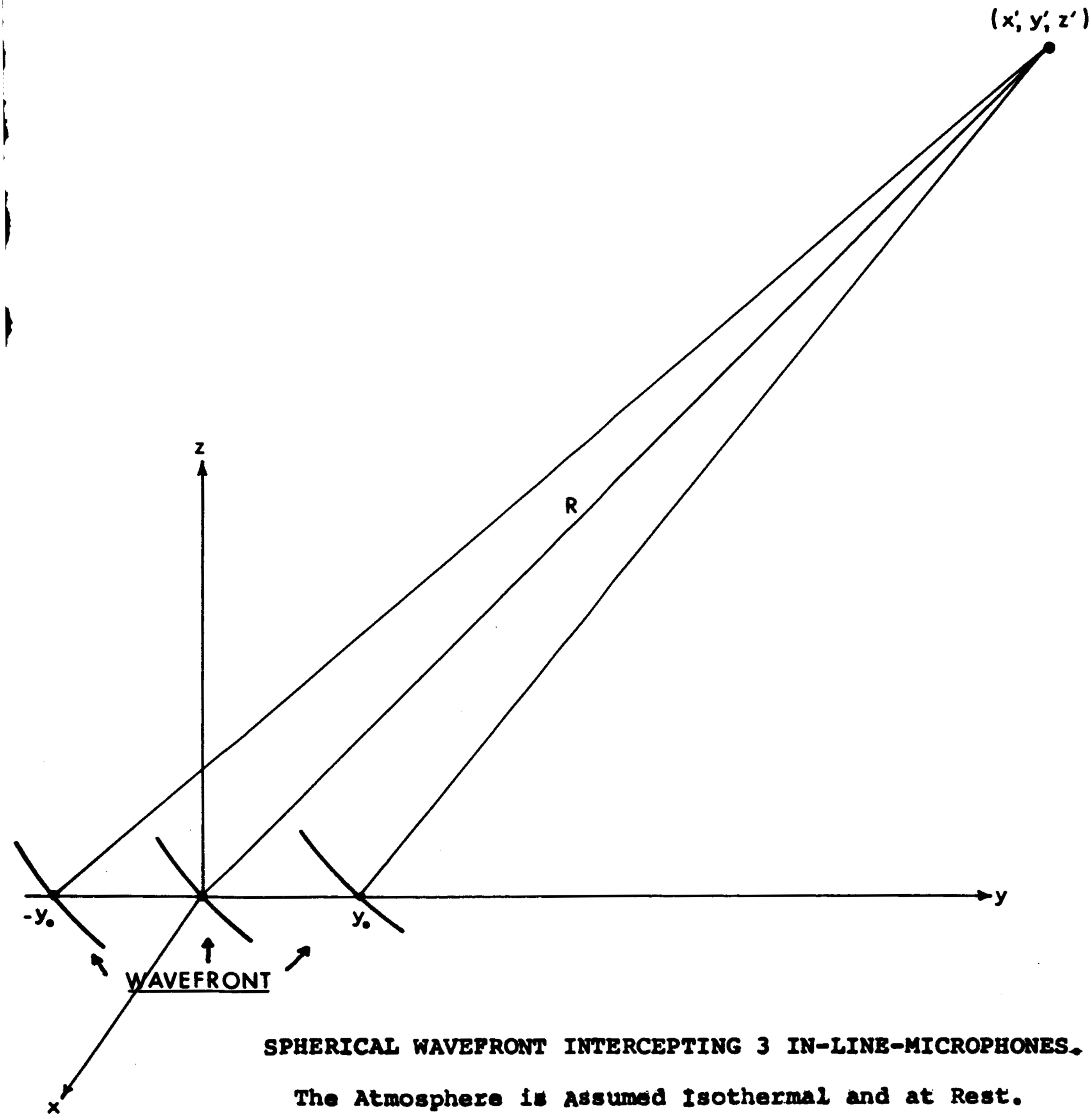

SPHERICAL WAVEFRONT INTERCEPTING 3 IN-LINE-MICROPHONES.

The Atmosphere is Assumed Isothermal and at Rest.

Fig. 14

Substituting $R^2 = x'^2 + y'^2 + z'^2$ and expanding the square roots

$$t_{-y_o} - t_{+y_o} = \frac{R}{V} [2y_o \frac{y'}{R^2} - \frac{y_o^3 y'}{R^4} + \ldots]$$

$$= \frac{2y'}{V} (\frac{y_o}{R}) - \frac{y'}{V} (\frac{y_o}{R})^3 + \ldots \qquad (40)$$

The first term is just the plane wave term. Note that the second order term in y_o/R is absent. This is due to the symmetrical use of the two microphones about the origin. This term always disappears if microphones are taken in such pairs. A three microphone array therefore could not be used in this manner and the error due to the non-plane wave would be correspondingly greater.

For the array used during the SA-9 launch y_o for the extreme microphones is about 600 meters. After the vehicle has reached maximum rawinsonde altitude R is at least 30,000 meters. In this case $y_o/R \approx 2 \times 10^{-2}$ and $(y_o/R)^3 \approx 8 \times 10^{-6}$. Since the time $t_{-y_o} - t_{+y_o}$ is on the order of 2 second, $\frac{2y'}{V} \approx 10^2$, so $\frac{y'}{V} \approx .5 \times 10^2$. The spherical term is then about 1/2 ms. Therefore this size array is compatible with the accuracy (1 ms) desired in the reading of microphone times.

VIII. CONCLUSION

The agreement between the wind profiles determined by the Rocket Exhaust Noise Wind Technique and other simultaneous measurements during the flight of the SA-9 is evidence of the validity of the acoustic technique described herein.

On the basis of the error analysis, the maximum errors in the SA-9 wind profile are estimated to be about $\pm$ 20m/s at 85Km. and decreasing to about $\pm$ 7m/s at 30Km. These errors are attributed principally to inaccuracies in the reading of the microphone arrival times and should be reducible to about $\pm$ 5m/s at 85 Km. to $\pm$ 2m/s at 30Km. by the use of improved data reduction techniques.

At locations where large booster rockets are launched regularly, a rather modest ground station can gather wind data from the ground to, in some cases, 85Km. These data measured concurrent with the rocket flight have important engineering value, and the upper atmosphere wind profiles measured on a regular basis would be an important supplement to the data available to meterologists.

REFERENCES

1) Nordberg, W., "A Method of Analysis for the Rocket-Grenade Experiment," U. S. Army Signal Engineering Laboratories Technical Memorandum NR. M-1856, February 1957.

2) Stroud, W. G., W. Nordberg, W. R. Bandeen, F. L. Bartman, and P. Titus, "Rocket-Grenade Measurements of Temperature and Winds in the Mesosphere over Churchill, Canada," J. Geophysical Research, 65, 2307-2323, 1960.

3) Stroud, W. G., Nordberg, W., and Walsh, J. R., "Temperatures and Winds between 30 and 80 km," J. Geophysical Research, 61, 45-56, 1956.

4) "Ground Support and Data Analysis and Associated Research and Development for the Rocket Grenade Experiment," Final Report, September 1962, Edited by A. M. Parra, Schellenger Research Laboratories, Texas Western College, El Paso, Texas.

5) Otterman, J., "A Simplified Method for Computing Upper-Atmosphere Temperature and Winds in the Rocket-Grenade Experiment," Univ. of Mich. Tech. Report 2387-40-T, Army Contract No. DA-36-039-SC-64657, June 1958.

6) Milne, E. A., "Sound Waves in the Atmosphere," Phil. Mag. 42, 96-114, 1921.